Feasibility study and preliminary test of a coded aperture based muonic X-ray element imaging method

Ziwen PAN(潘子文), Zebin LIN (林泽斌), Bangjiao YE (叶邦角)

State Key Laboratory of Particle Detection and Electronics, USTC

6th Nov. 2023

Workshop on Muon Science Technology and Industry (MELODY 2023)

Outline

I Introduction to muonic X-rays

II Simulation on coded aperture imaging

III Preliminary tests with gamma rays

IV Summary and outlook


I. Introduction to muonic X-rays

1.1 Physical nature of muons

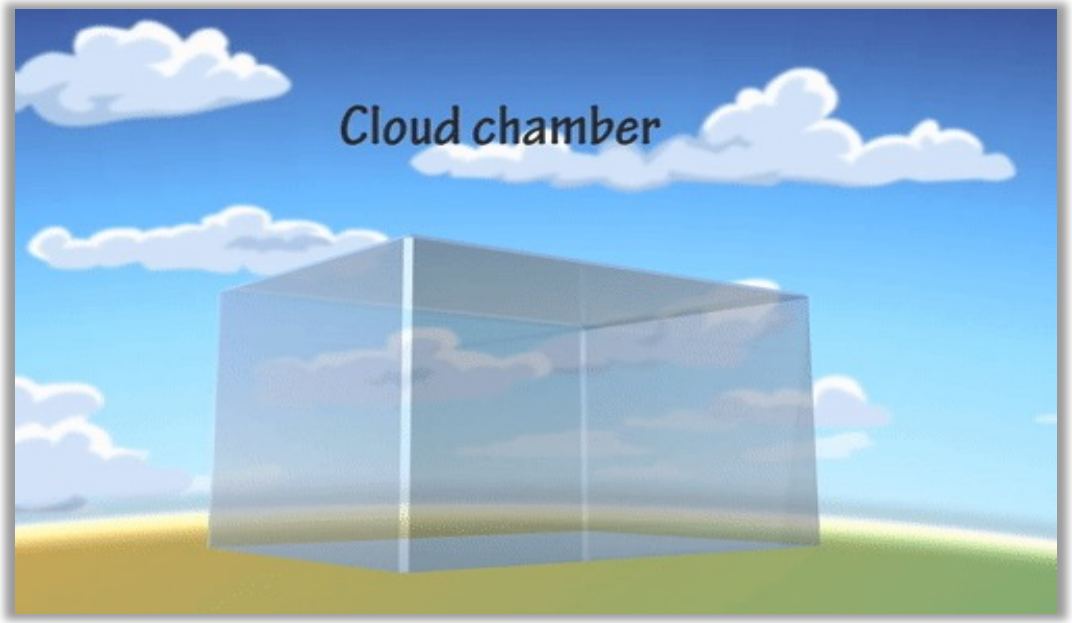

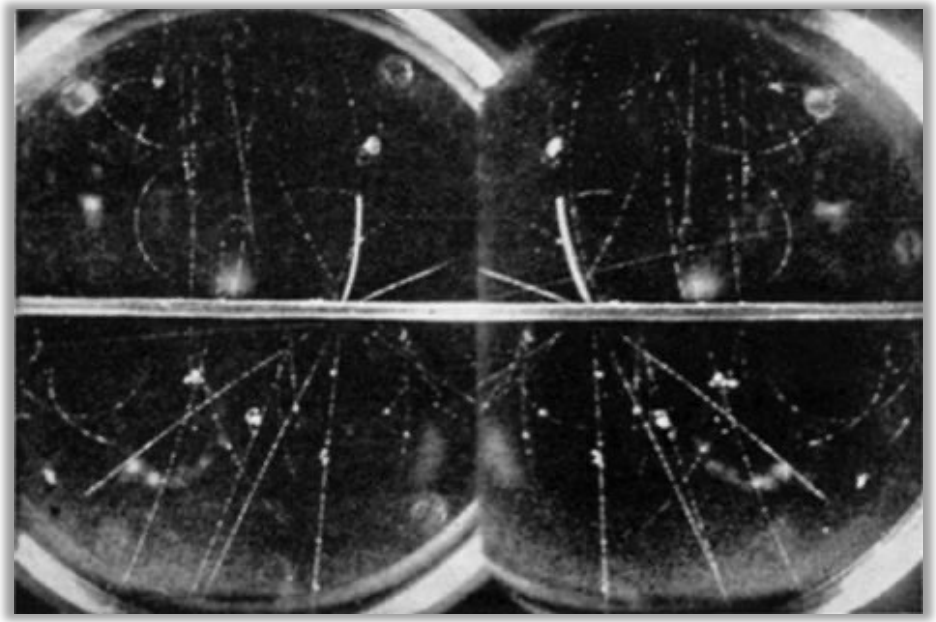

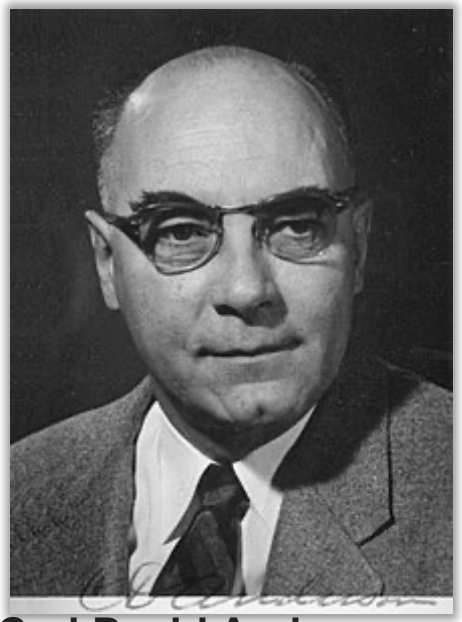

Carl David Anderson
(1905-1991)

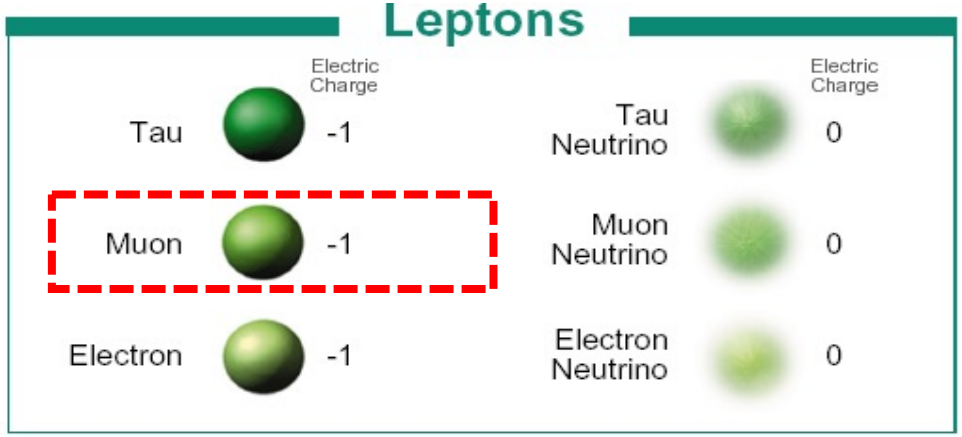

	charge	spin	mass	moment	$\gamma / 2\pi$ (kHz G^{-1})	lifetime (μs)
e	$\pm$e	1/2	m_e = 0.51 MeV	657 μ_p	2800	∞
μ	$\pm$e	1/2	207 m_e = 105.7 MeV	3.18 μ_p	13.5	2.19
p	$\pm$e	1/2	1836 m_e = 938 MeV	μ_p	4.26	∞

1.2 Generation of negative muon beams

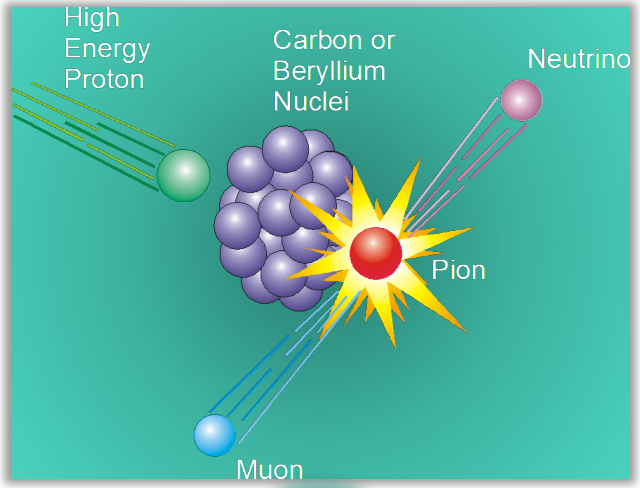

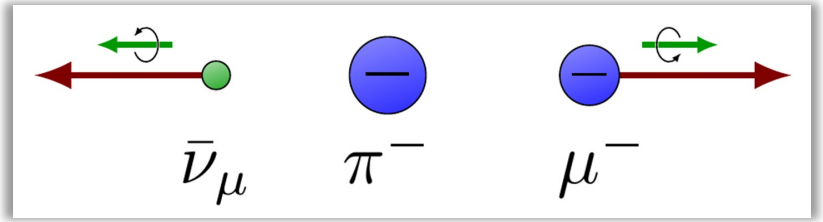

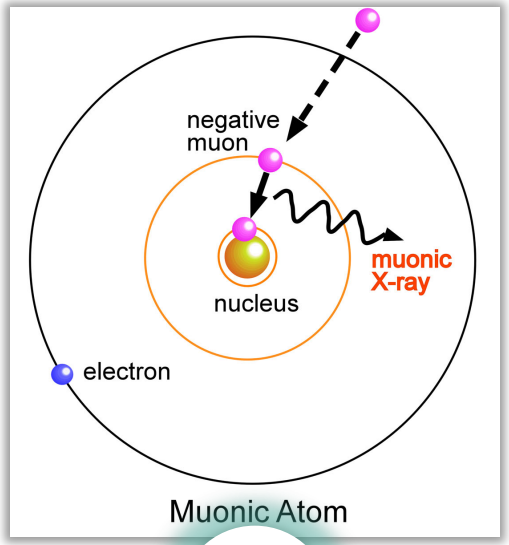

Target → **π^-** → **μ^-**

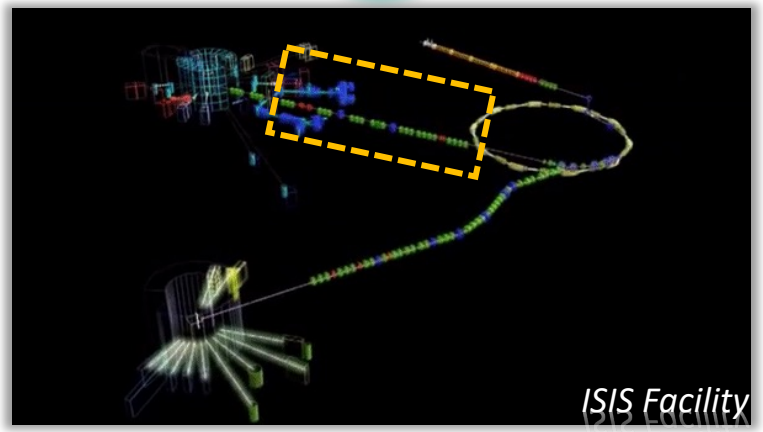

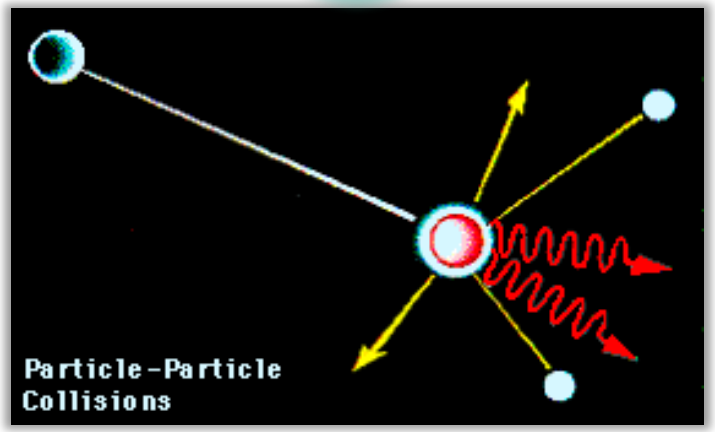

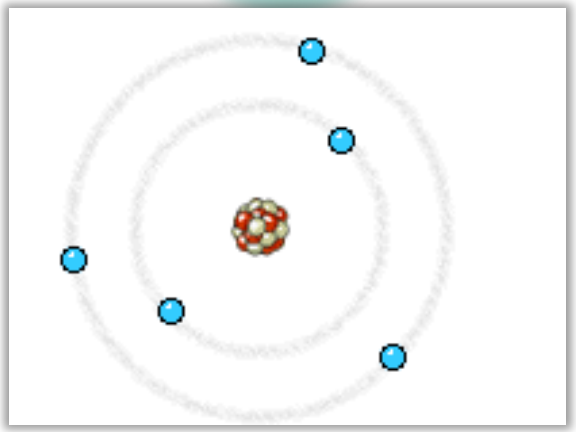

1.3 Processes of muonic X-ray emission

Muon Induced X-ray Emission (MIXE)

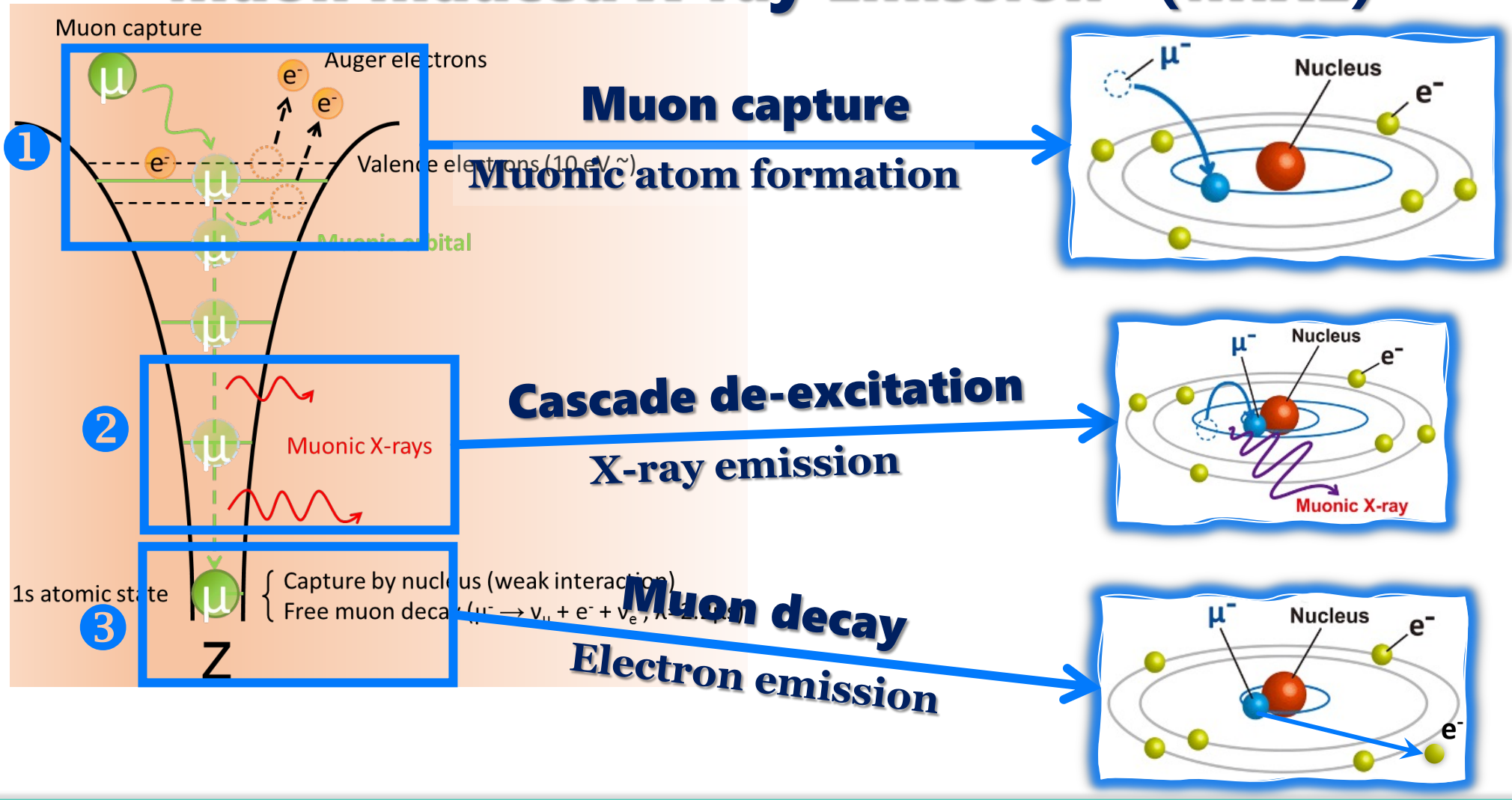

1.4 Advantages of MIXE method

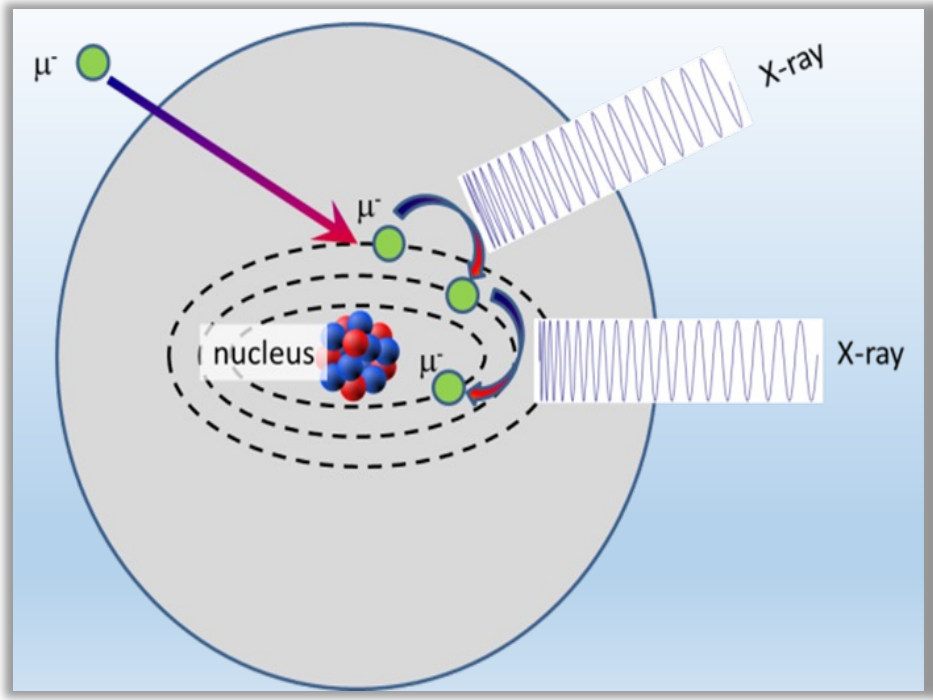

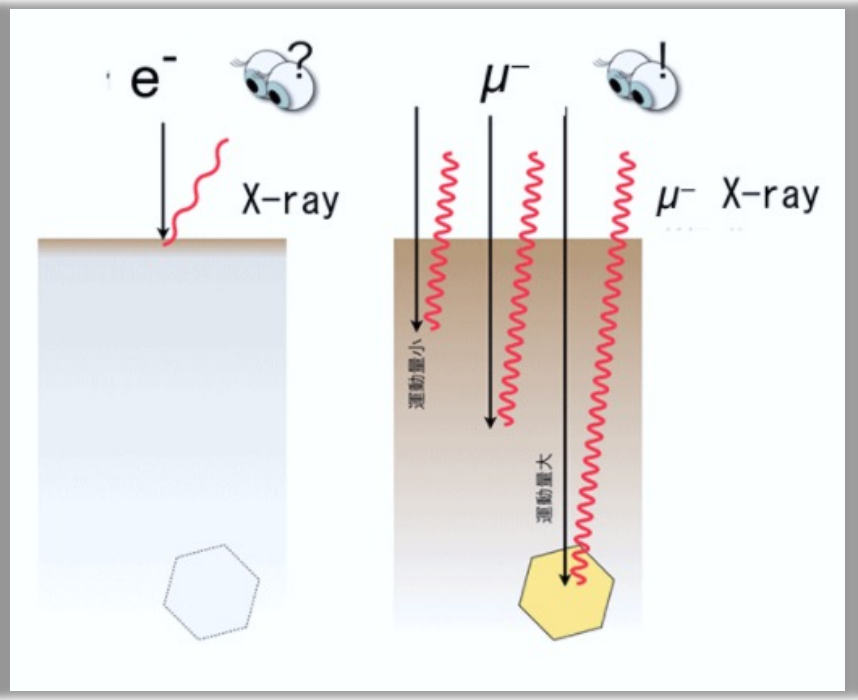

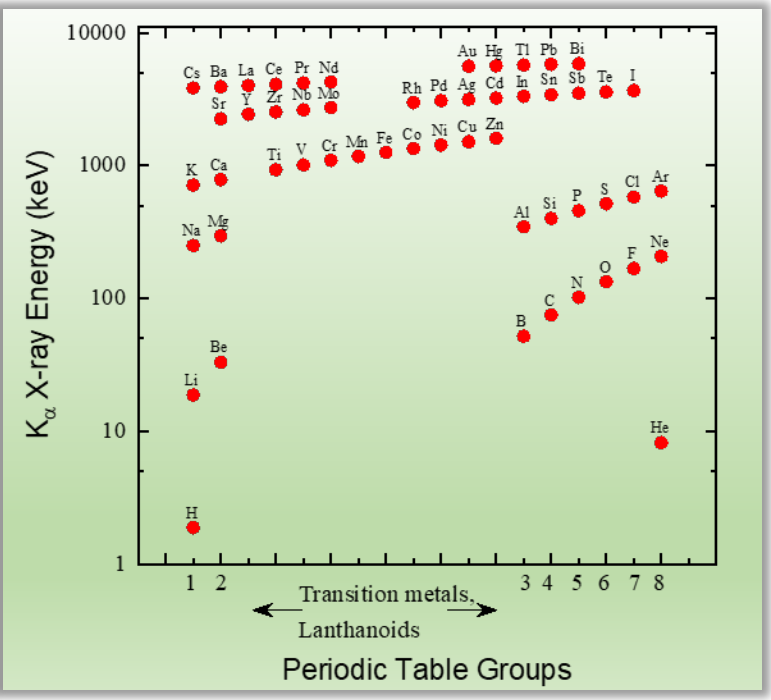

- **High energy, high penetrating capability** (~200 times of electrons, induced X-rays with an energy in 10s keV – 10MeV)
- **Energy dependency on atomic number** (multiple atoms/elements distinguishable at one time)
- **Better sensitivity to low-Z materials** (high X-ray energy that can be responded by detectors)
- **Adjustable muon beam momentum** (depth analysis of elemental distributions)
- **Non-destructive measurement** (no radiation risk to materials)

1.5 Multi-field applications

Meteorite

Cultural heritage

Li-ion battery

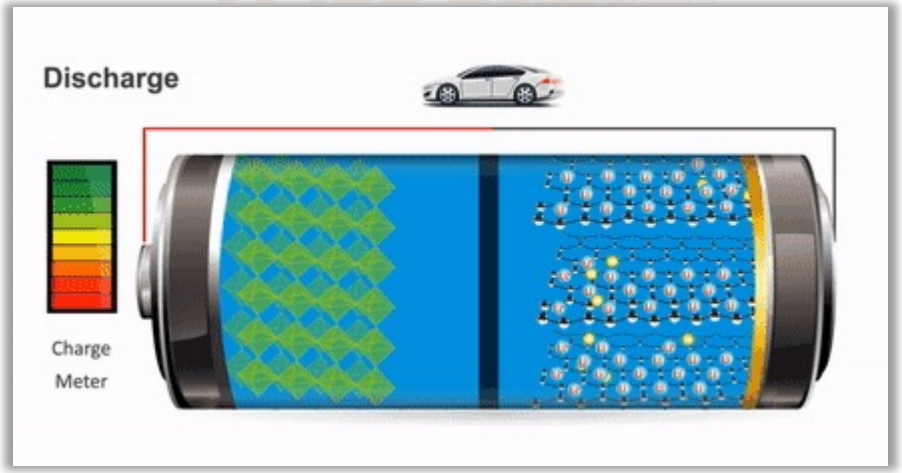

Biomaterials

Isotope analysis

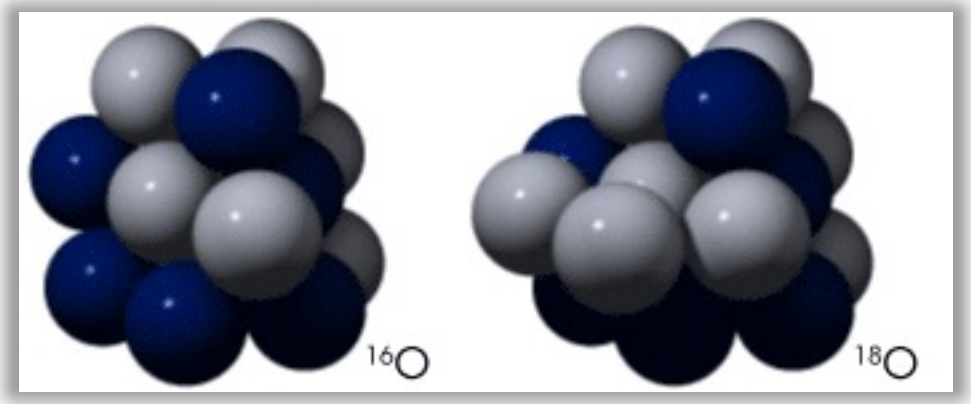

……

Handbook of Cultural Heritage Analysis, Chapter 3

1.6 Instruments at muon facilities

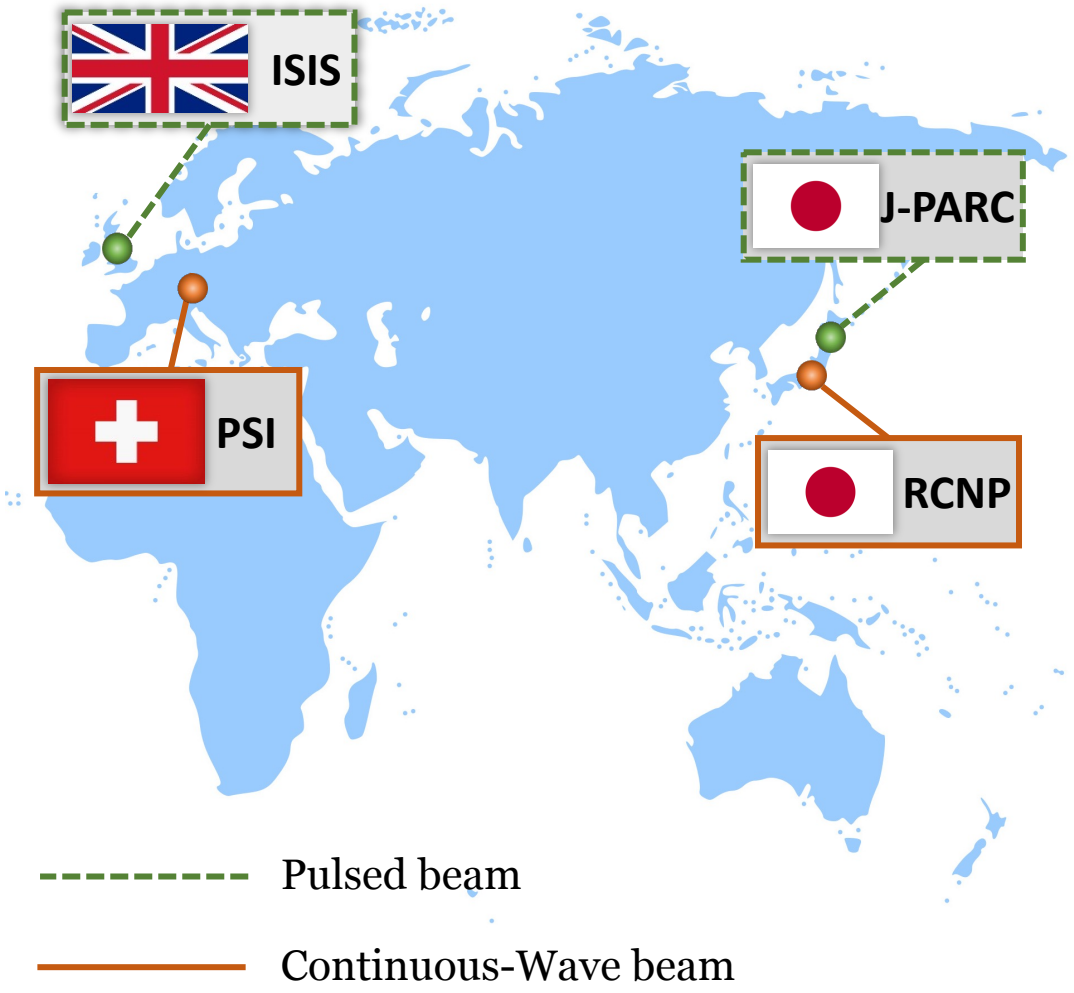

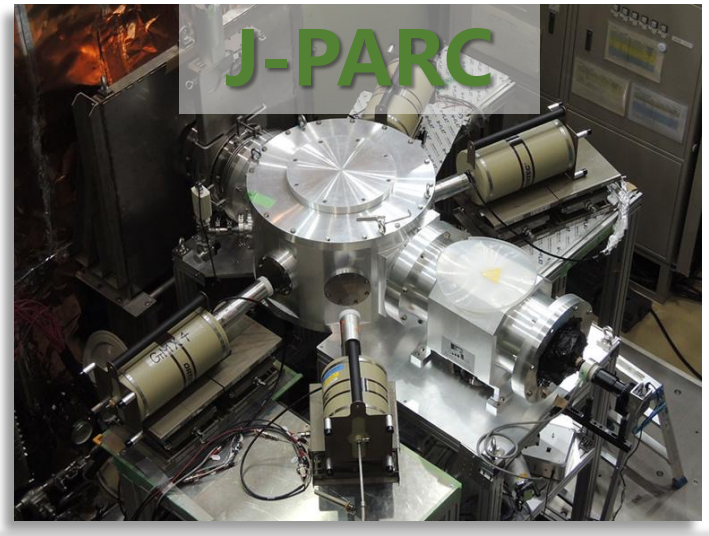

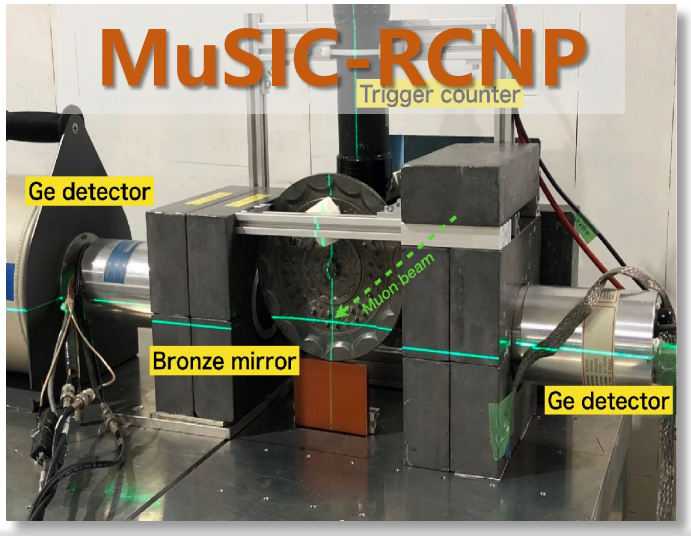

II. Simulation on coded aperture imaging

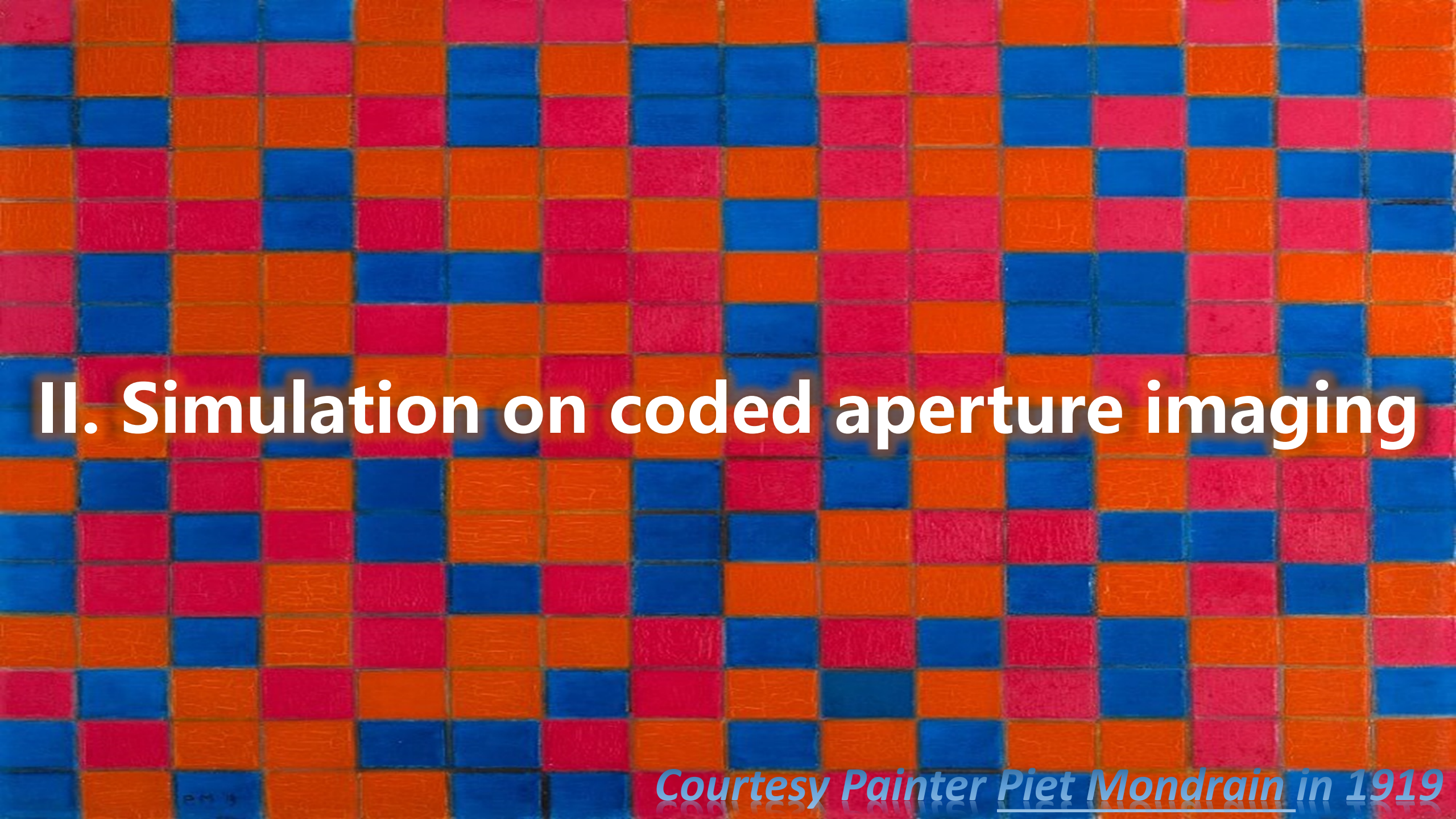

Courtesy Painter Piet Mondrain in 1919

2.1 Existing imaging methods

Direct imaging

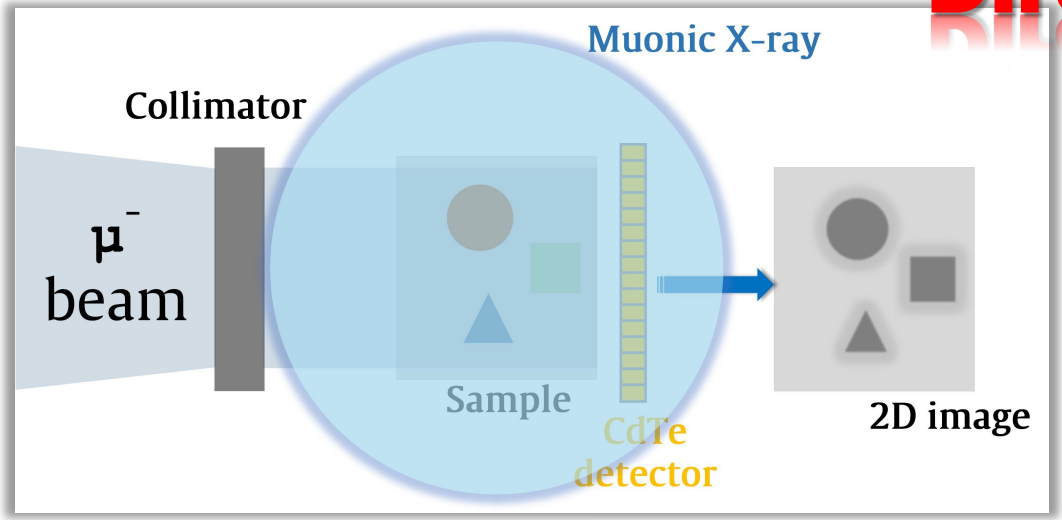

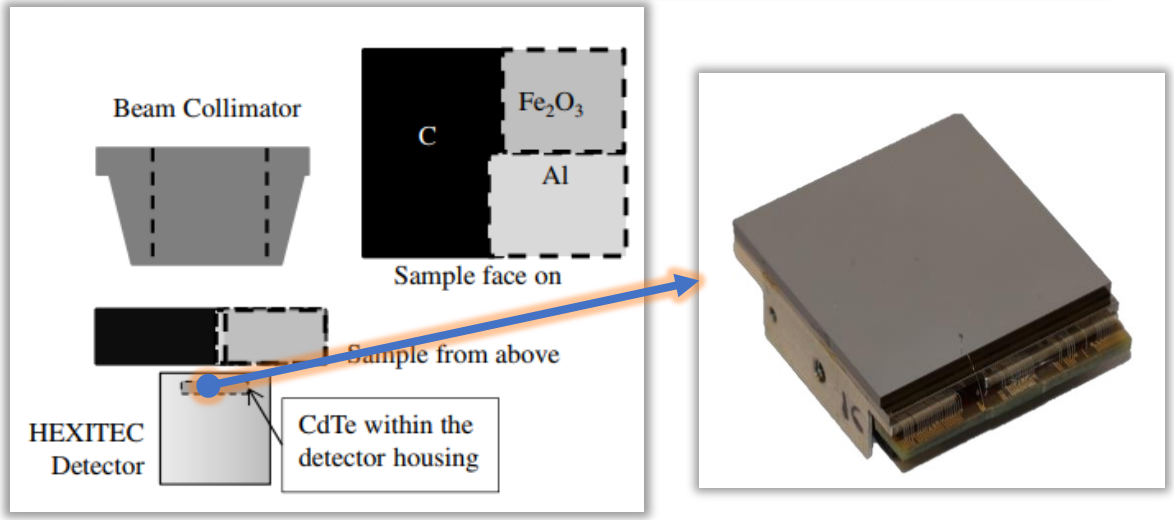

Science and Technology Facilities Council
ISIS Neutron and Muon Source

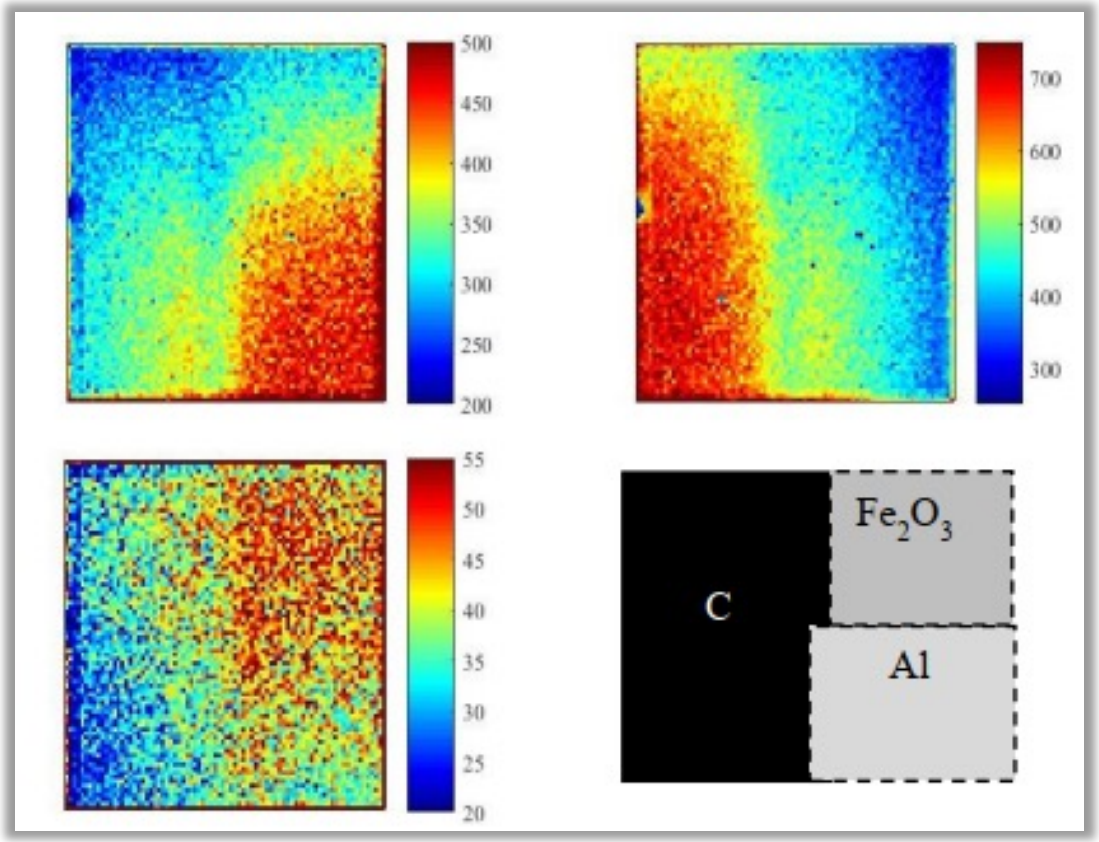

A. Hillier, et al., JPS Conf. Proc. 21, 011042 (2018)

2.1 Existing imaging methods

Pinhole imaging

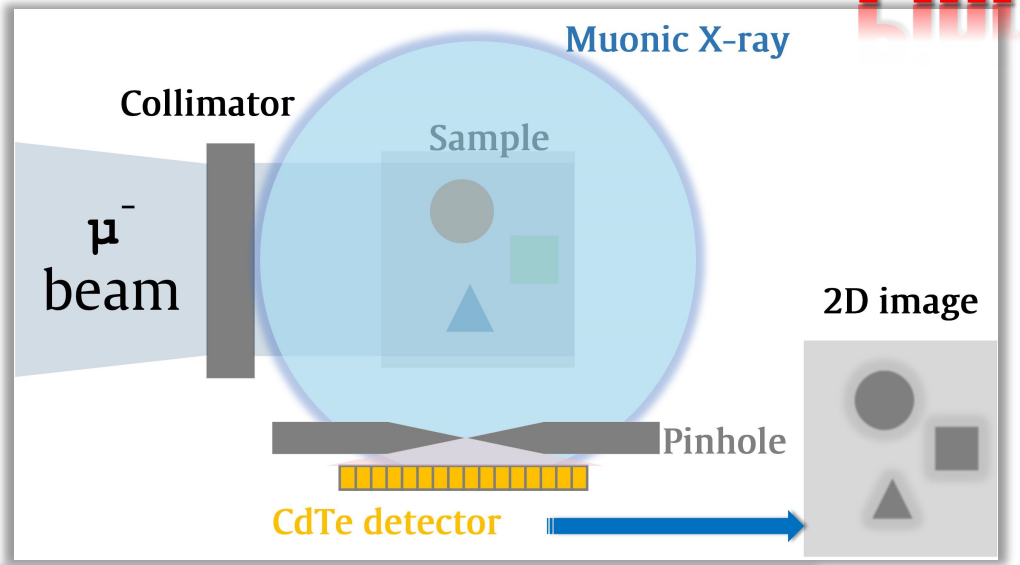

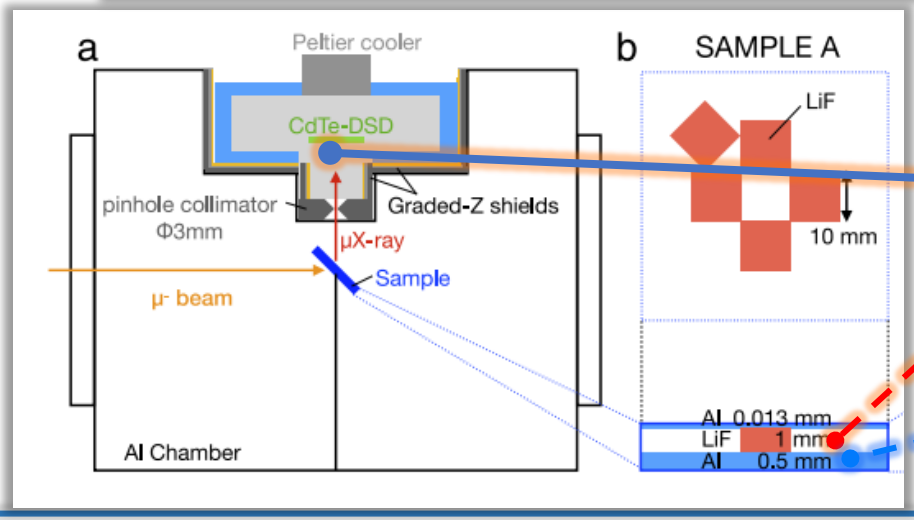

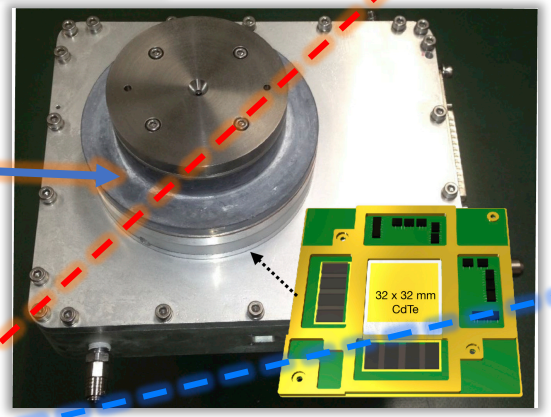

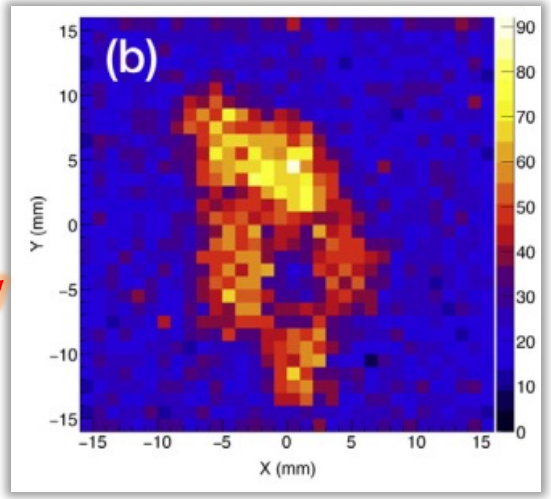

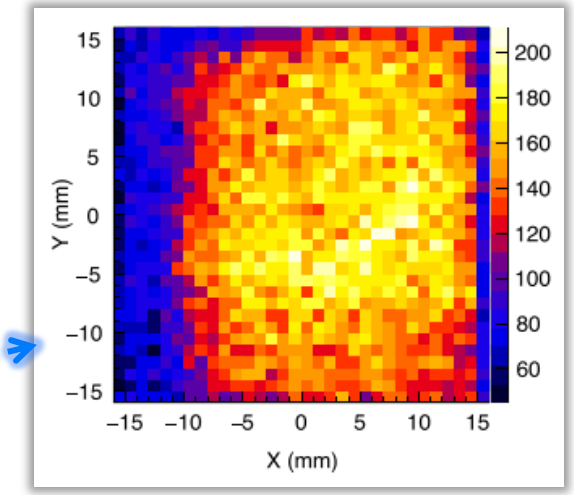

M. Katsuragawa et al., NIMA 912 (2018) 140

Pinhole imaging + CT

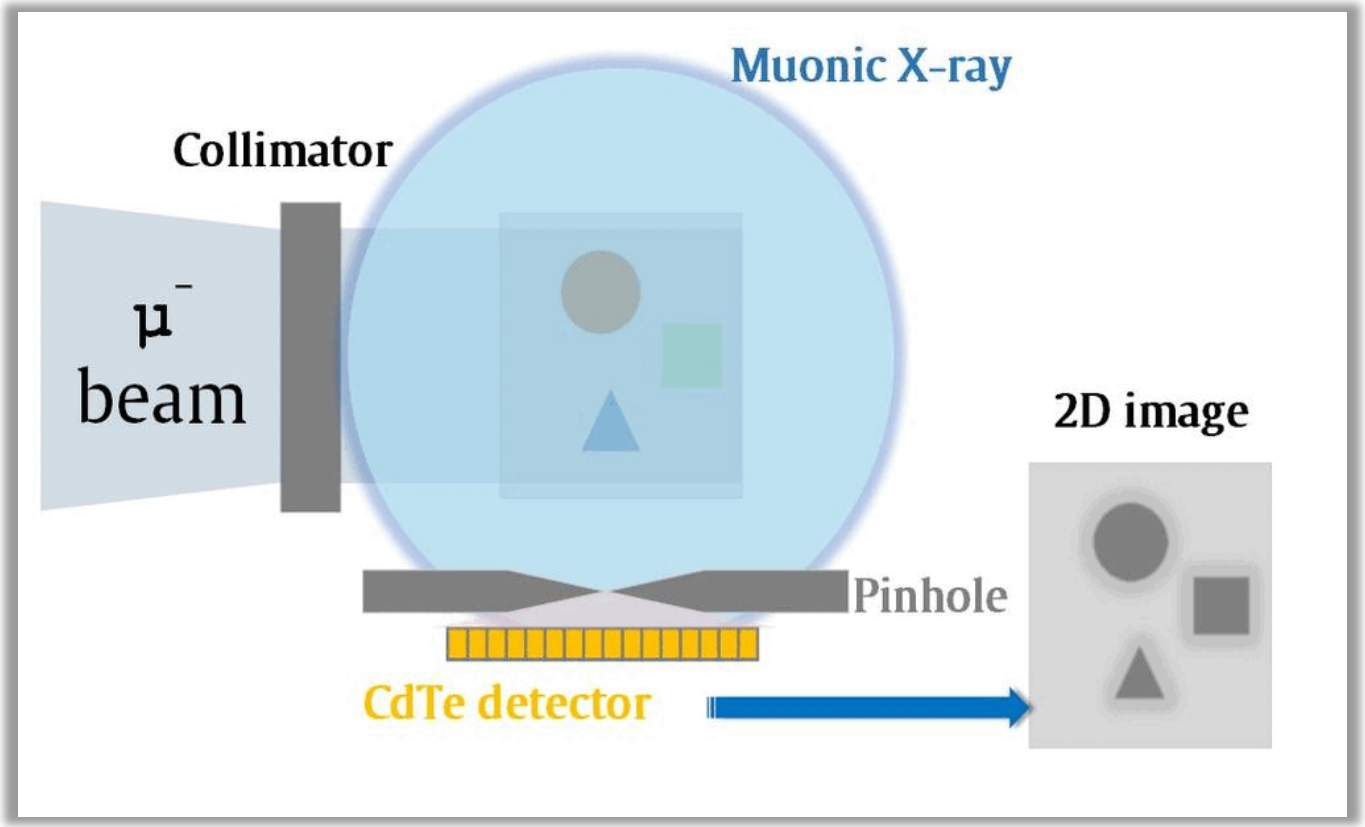

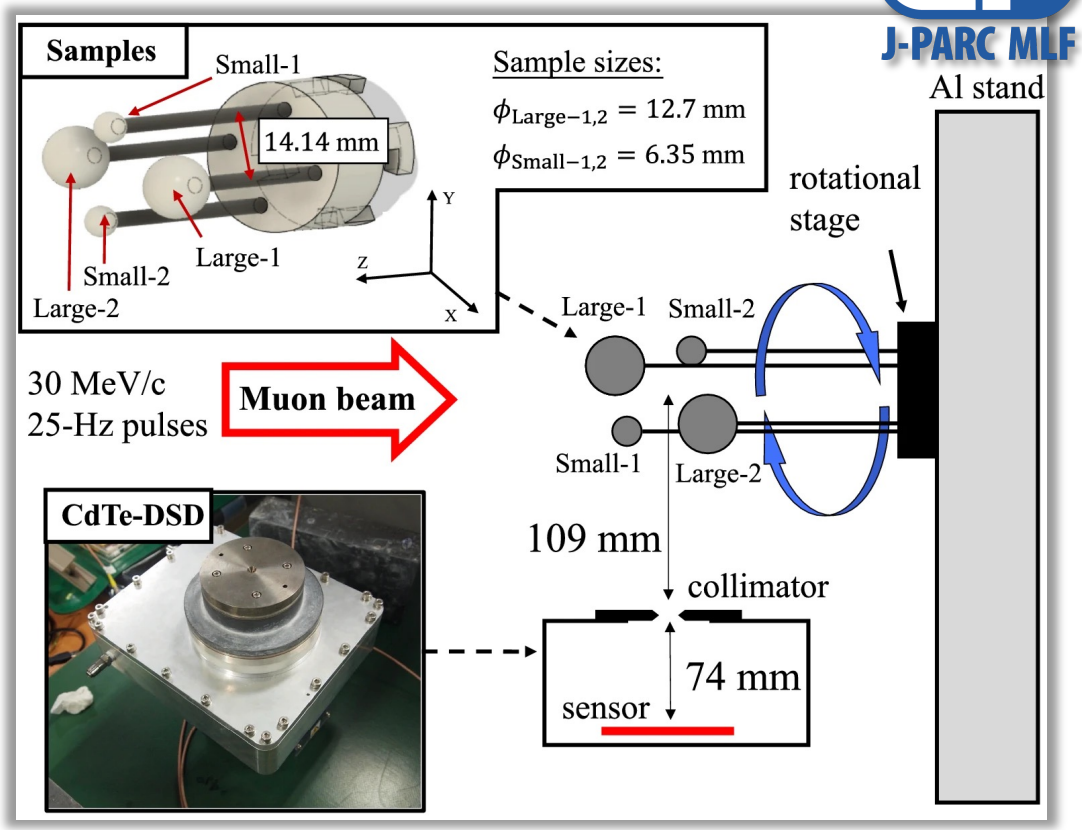

J-PARC MLF

I. Chiu et al., Sci. Rep. 12 (2022) 5261

2.1 Existing imaging methods

Pinhole imaging + CT

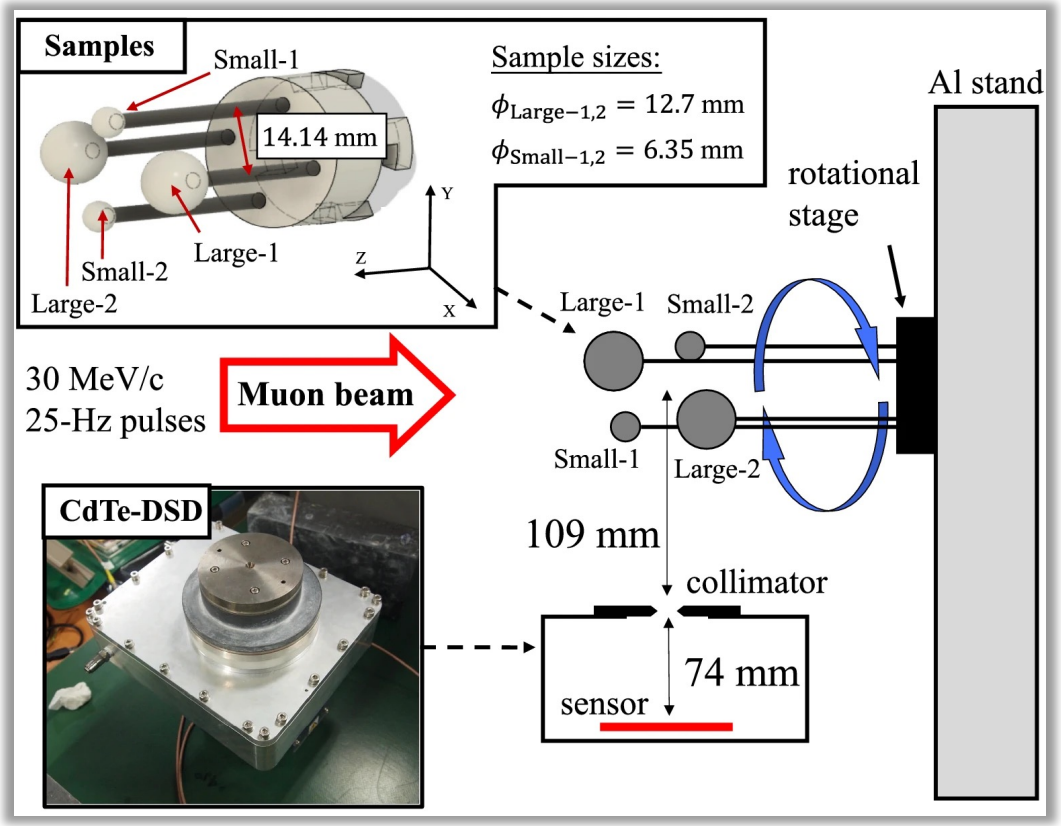

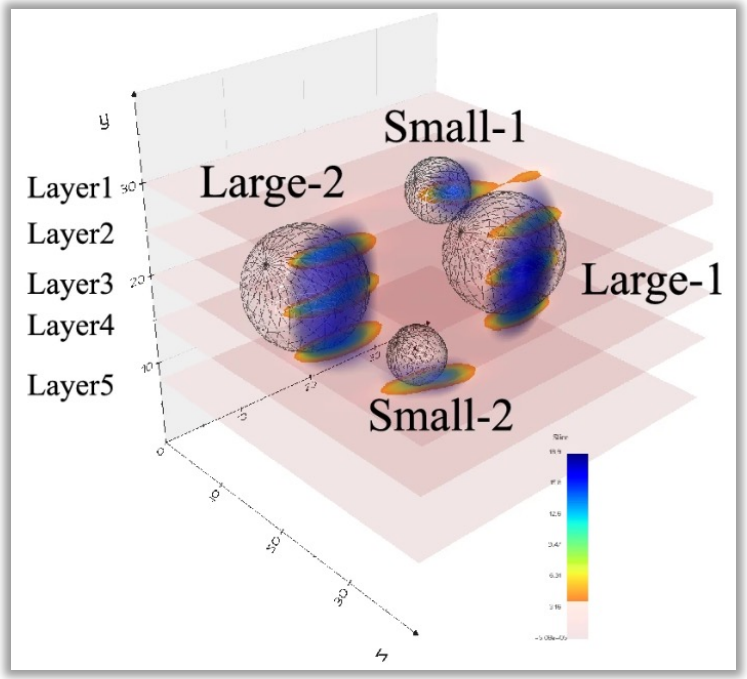

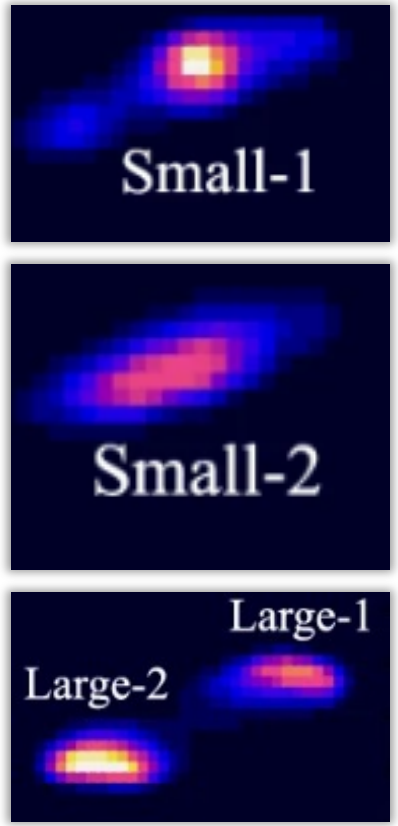

I. Chiu et al., Sci. Rep. 12 (2022) 5261

2.2 Coded aperture (multi-pinhole) imaging

Direct imaging: high noise / high efficiency

Pinhole imaging: low noise / low efficiency

high efficiency

low noise

Coded aperture imaging

Modified Uniformly Redundant Array (**MURA**) coded mask

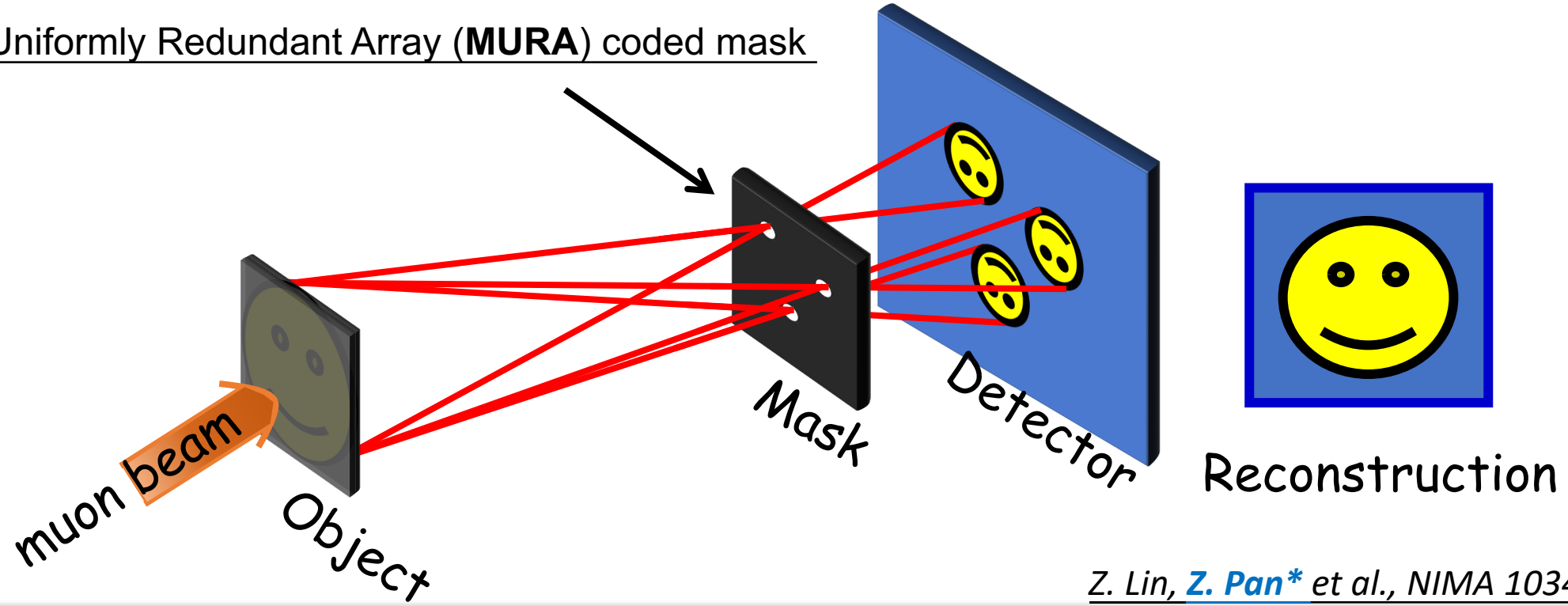

Z. Lin, Z. Pan et al., NIMA 1034 (2022) 166783*

2.3 Modelling in Geant4

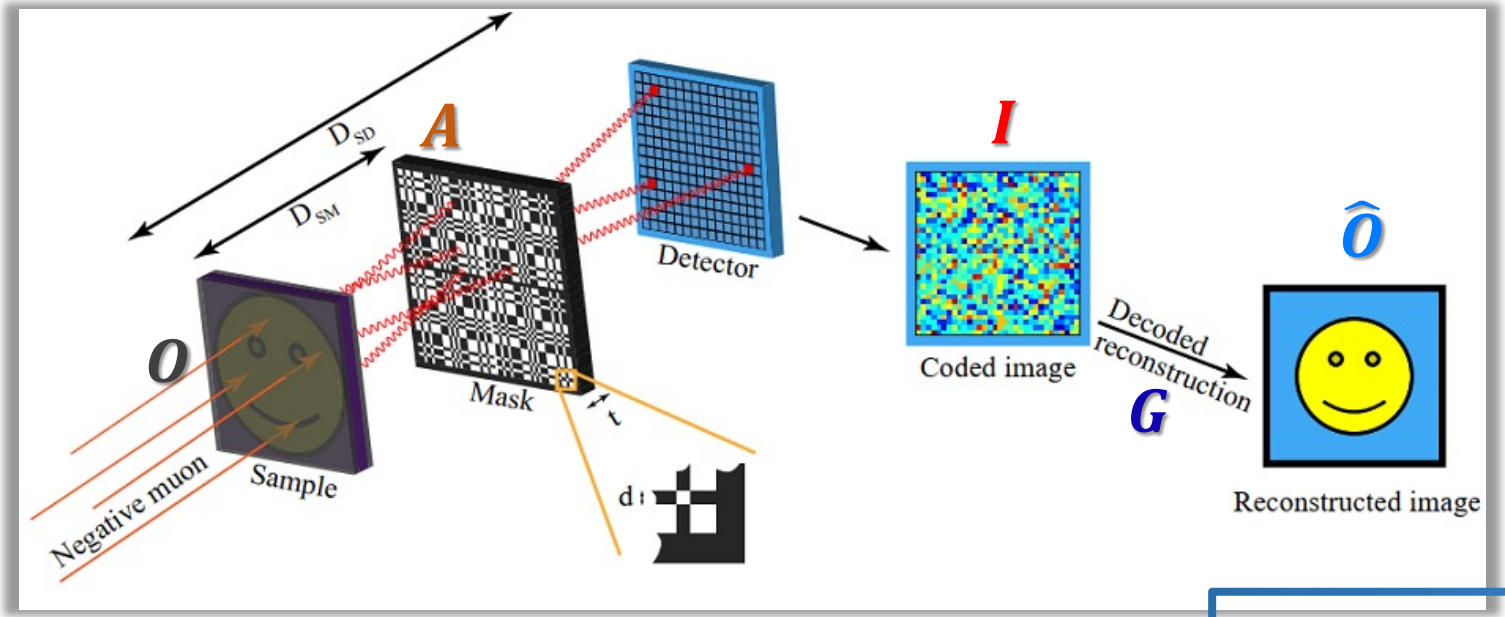

- **Muon**: 32.9 MeV/c @ 32×32 mm²
- **Sample**: 31×31×2 mm³
- **Coded mask**: MURA array 61×61 pixels
- **Detector**: CdTe detector
  - 32×32 mm² with 128 pixels
  - cell size in 0.25×0.25 mm²
  - 1.06% in energy resolution

$$I = O * A + N$$

$$A \otimes G = \delta$$

$$A = \begin{cases} 1, \text{hole} \\ 0, \text{wall} \end{cases} \qquad G = \begin{cases} 1, \text{hole} \\ -1, \text{wall} \end{cases}$$

$$\hat{O} = I \otimes G = O + N \otimes G \approx O$$

O: matrix of the sample
A: matrix of the coded mask
I: matrix of detected image (raw data)
G: decoding matrix of the coded mask
Ô: matrix of reconstructed imaging
N: matrix of background

Z. Lin, Z. Pan et al., NIMA 1034 (2022) 166783*

2.3 Modelling in Geant4

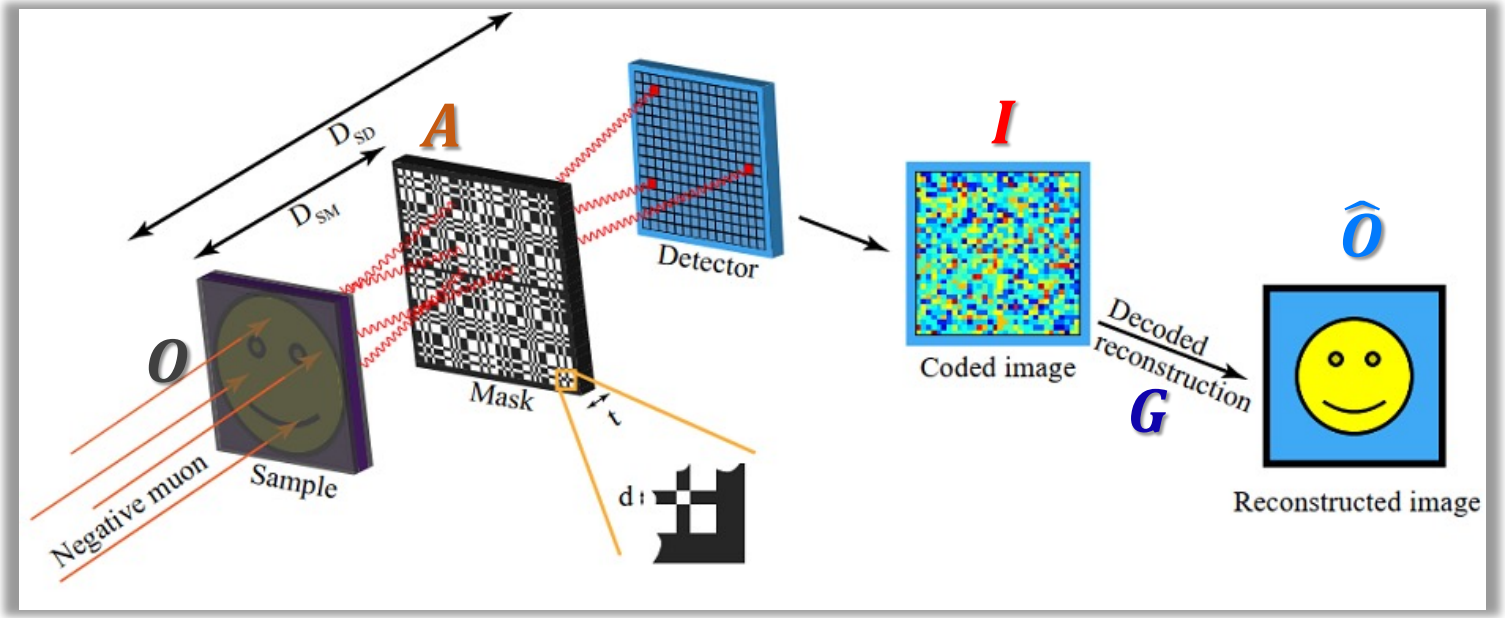

- **Muon**: 32.9 MeV/c @ 32×32 mm²
- **Sample**: 31×31×2 mm³
- **Coded mask**: MURA array 61×61 pixels
- **Detector**: CdTe detector
  32×32 mm² with 128 pixels
  cell size in 0.25×0.25 mm²
  1.06% in energy resolution

$$I = O * A + N$$

$$A \otimes G = \delta$$

$$A = \begin{cases} 1, \text{hole} \\ 0, \text{wall} \end{cases} \qquad G = \begin{cases} 1, \text{hole} \\ -1, \text{wall} \end{cases}$$

$$\hat{O} = I \otimes G = O + N \otimes G \approx O$$

Imaging quality: $$Q = \frac{2\mathrm{cov}\left(O, \hat{O}\right)}{\mathrm{var}\left(O\right) + \mathrm{var}\left(\hat{O}\right)} \frac{2\bar{O} \cdot \bar{\hat{O}}}{\bar{O}^2 + \bar{\hat{O}}^2}$$

Detection rate: $$\varepsilon = \frac{N_{D,X-ray}}{N_{Tot,muon}}$$

Figure of merit: $$FoM = Q/|\ln(\varepsilon)|$$

Z. Lin, Z. Pan et al., NIMA 1034 (2022) 166783*

2.3 Modelling in Geant4

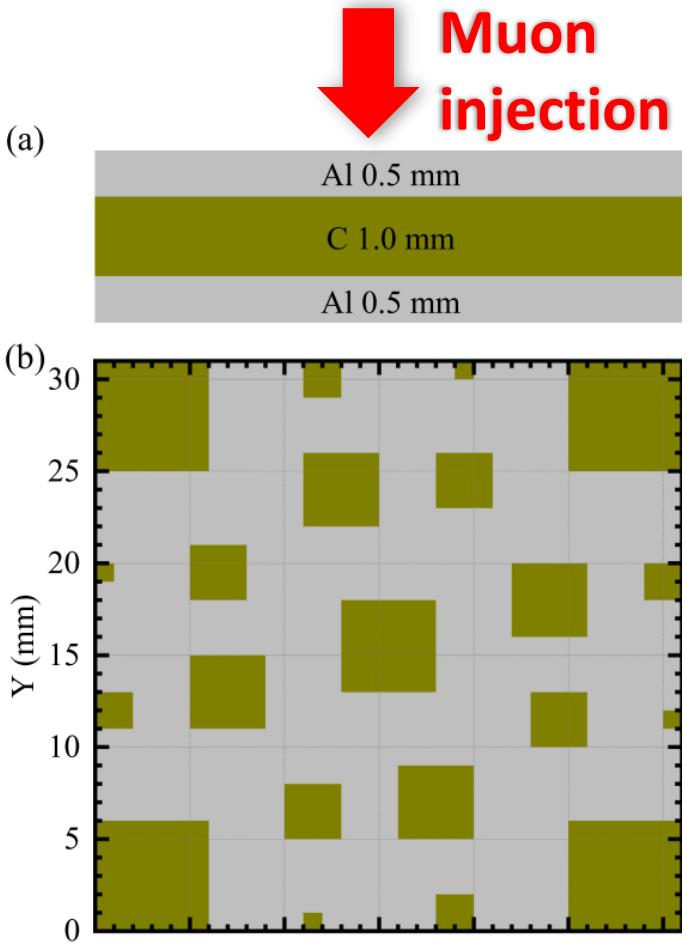

Implantation profile

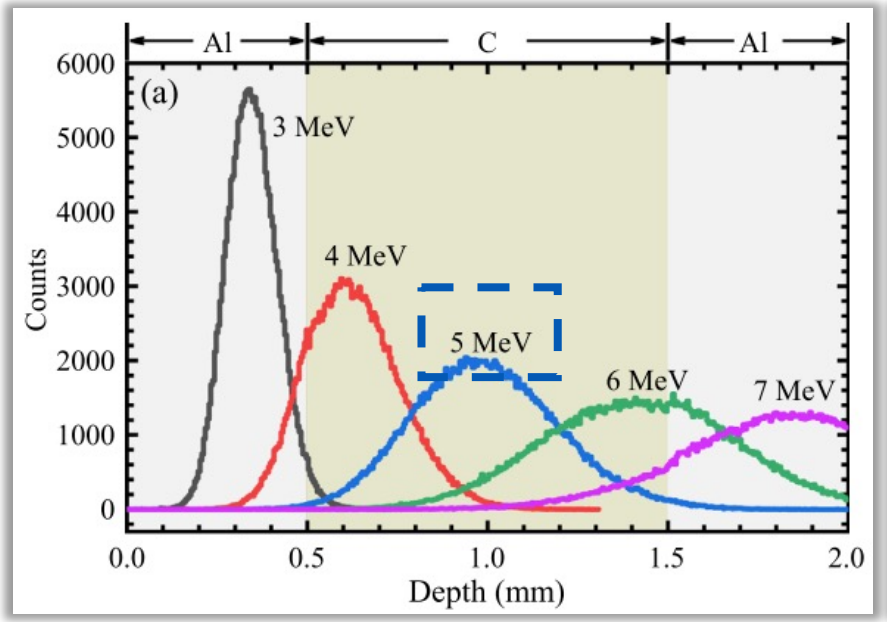

Muonic X-ray energy

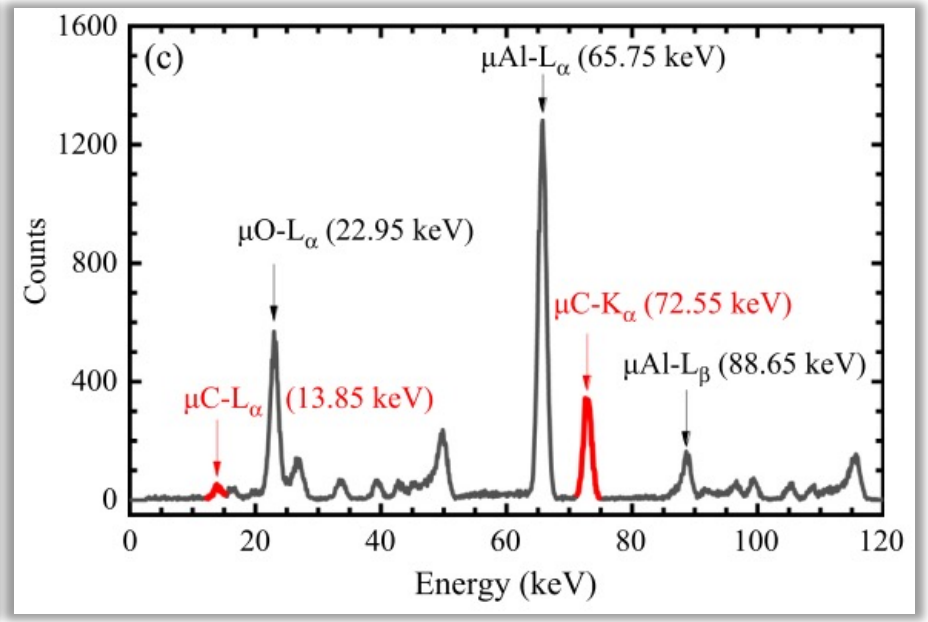

5 MeV = 32.9 MeV/c

Z. Lin, Z. Pan et al., NIMA 1034 (2022) 166783*

2.4 Results and comparison

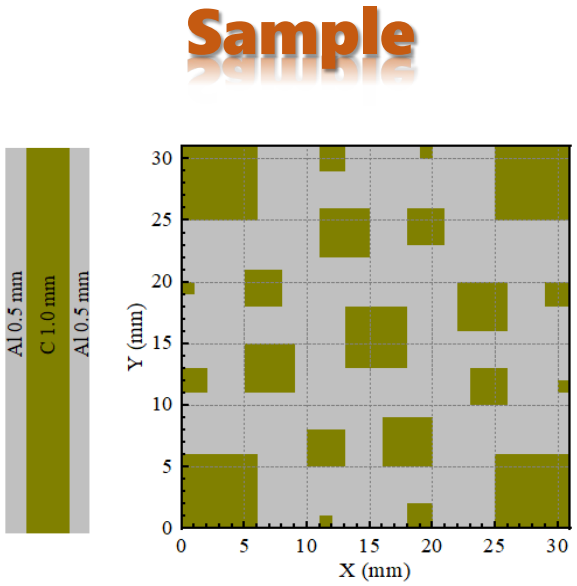

Imaging technique	Distance[Sample, Det]	Aperture size	Thickness	Q	ε	FoM
Coded aperture	80 mm	0.75 mm	1.0	0.670	1.25×10^{-3}	0.100
Single pinhole	80 mm	0.75 mm	20.0	0.649	2.06×10^{-5}	0.060
	80 mm	1.50 mm	20.0	0.381	2.67×10^{-5}	0.036

Z. Lin, Z. Pan et al., NIMA 1034 (2022) 166783*

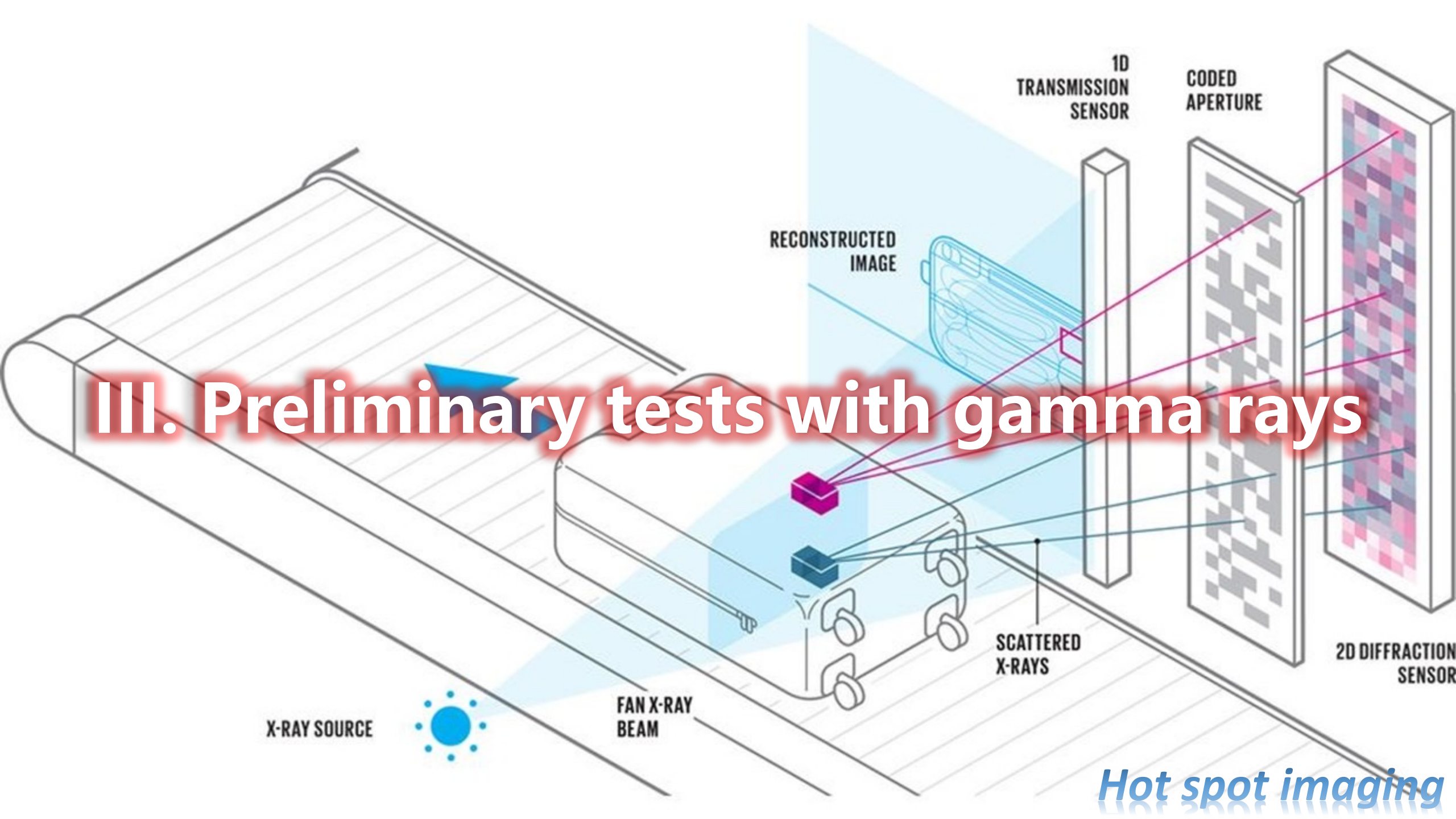

III. Preliminary tests with gamma rays

Hot spot imaging

3.1 Experimental configuration

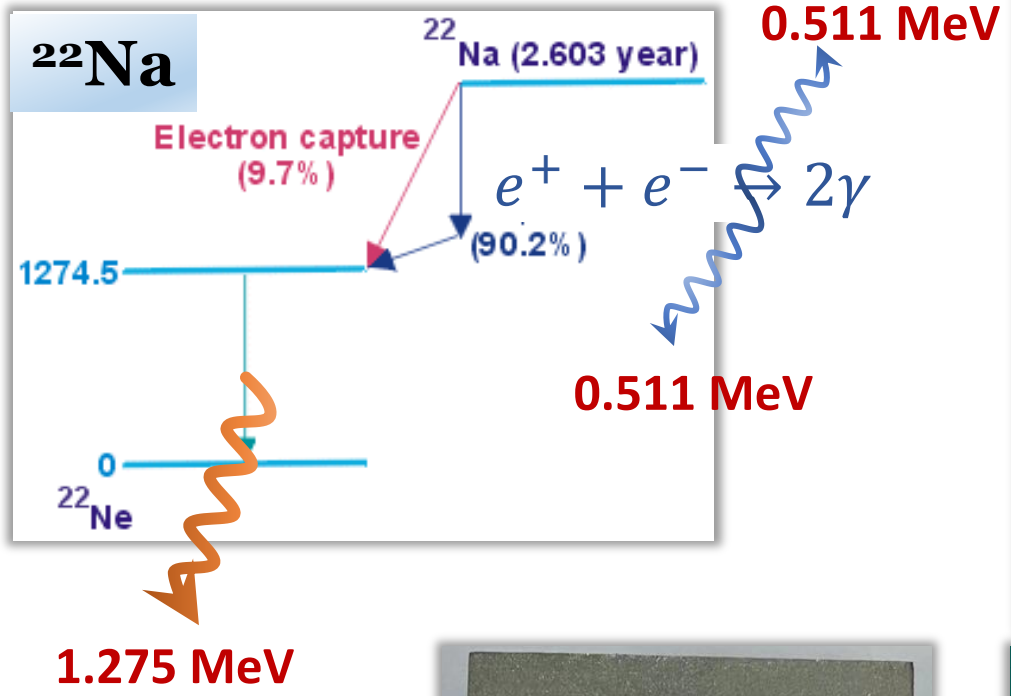

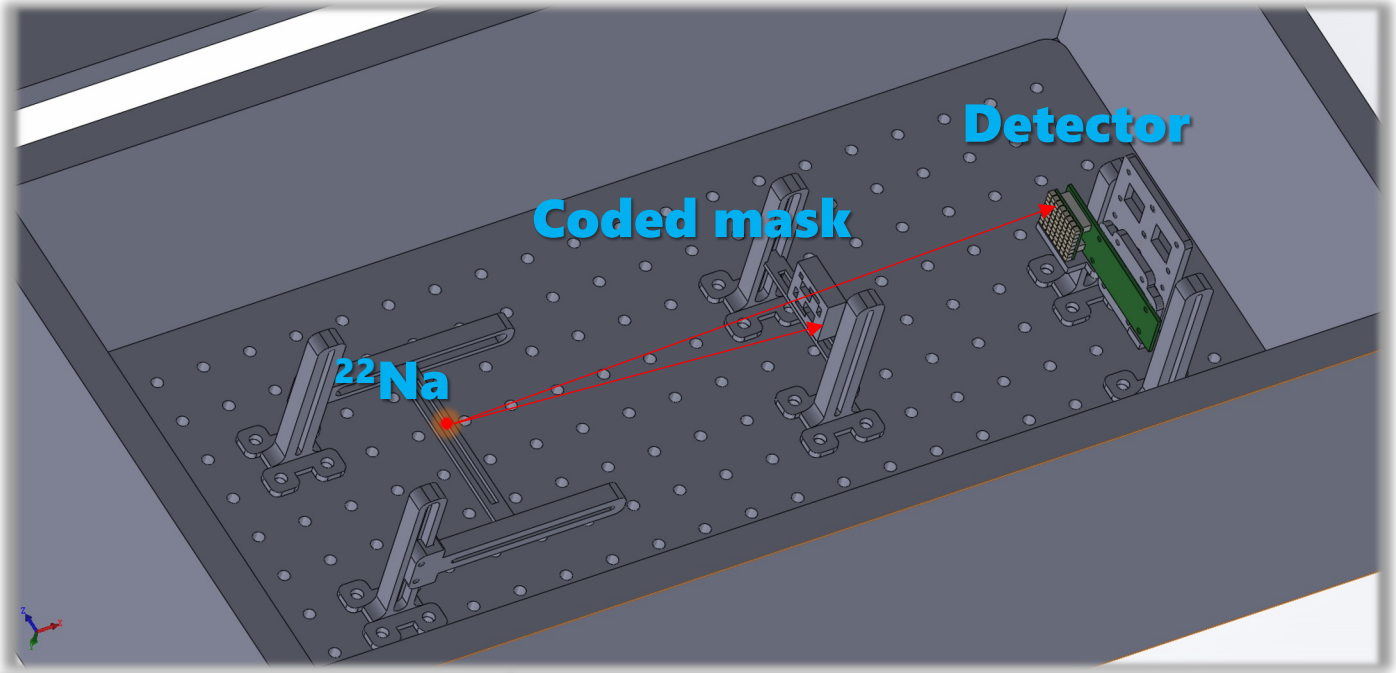

LYSO:
- Cerium-doped
- Lutetium
- Yttrium
- Orthosilicate

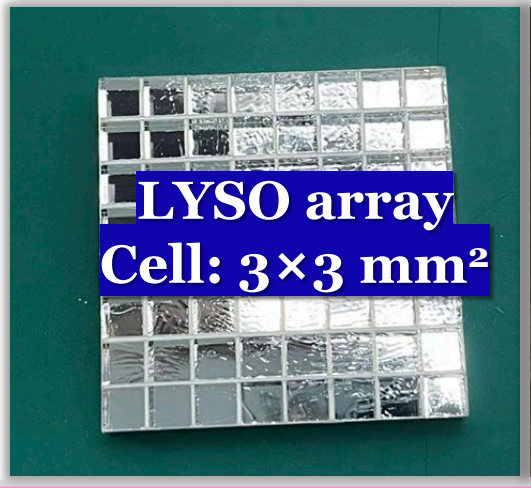

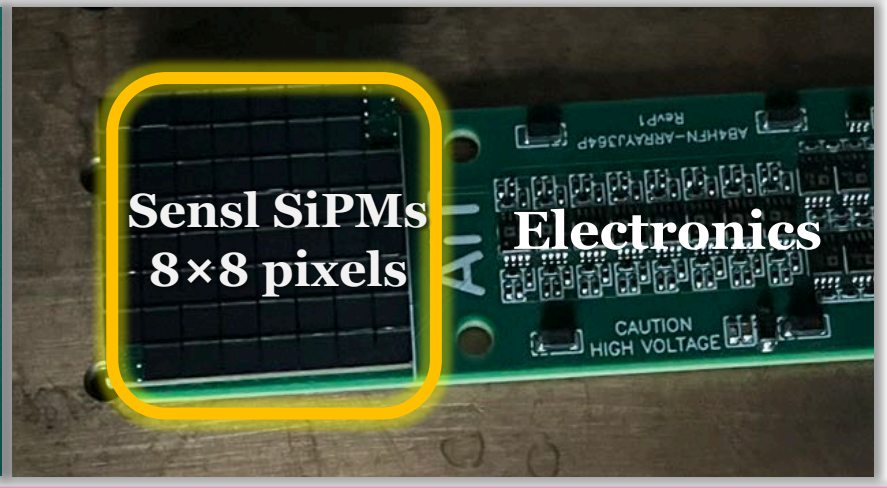

3.1 Experimental configuration

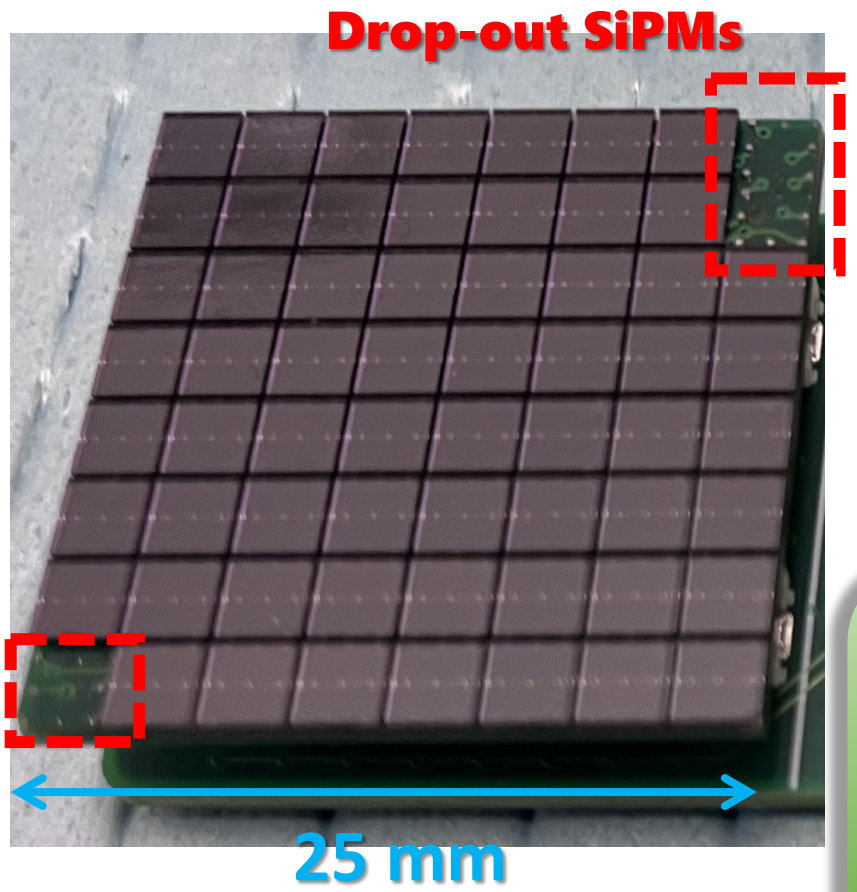

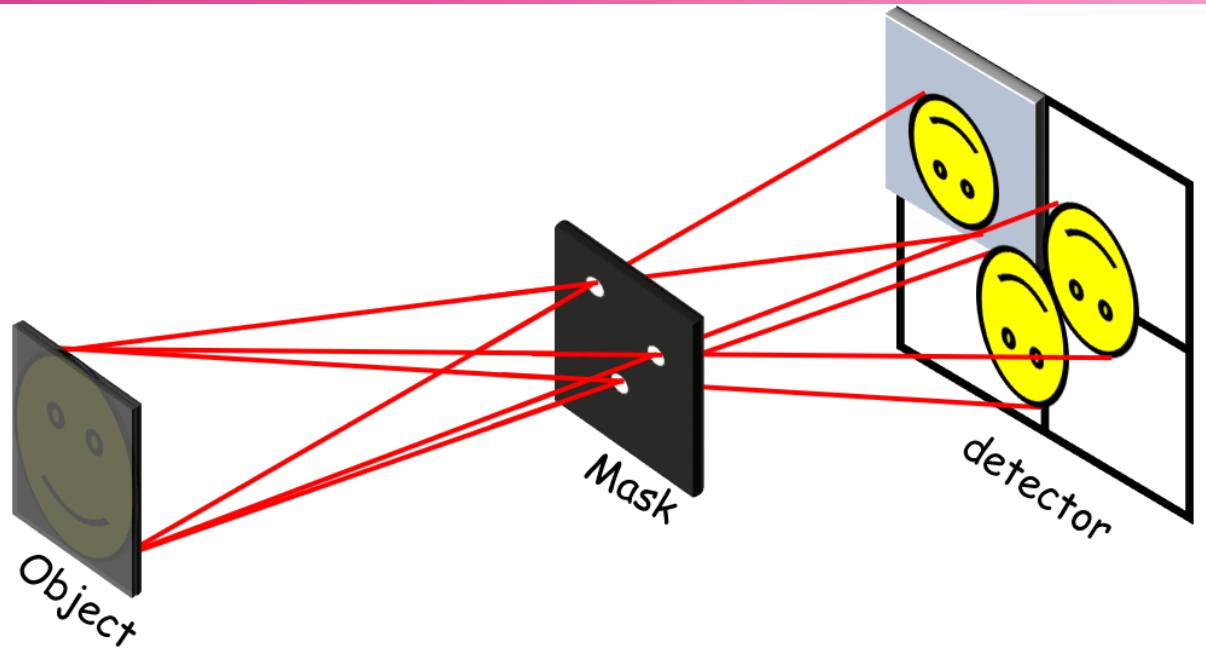

- As three SiPM pixels dropped out, only a 7×7 detector array can be used!
- The order of a MURA mask should be a prime number! It matches the detector we have.
- The detector was placed and measured at four neighboring locations to mimic a 14×14 array.

3.2 Single-source measurement

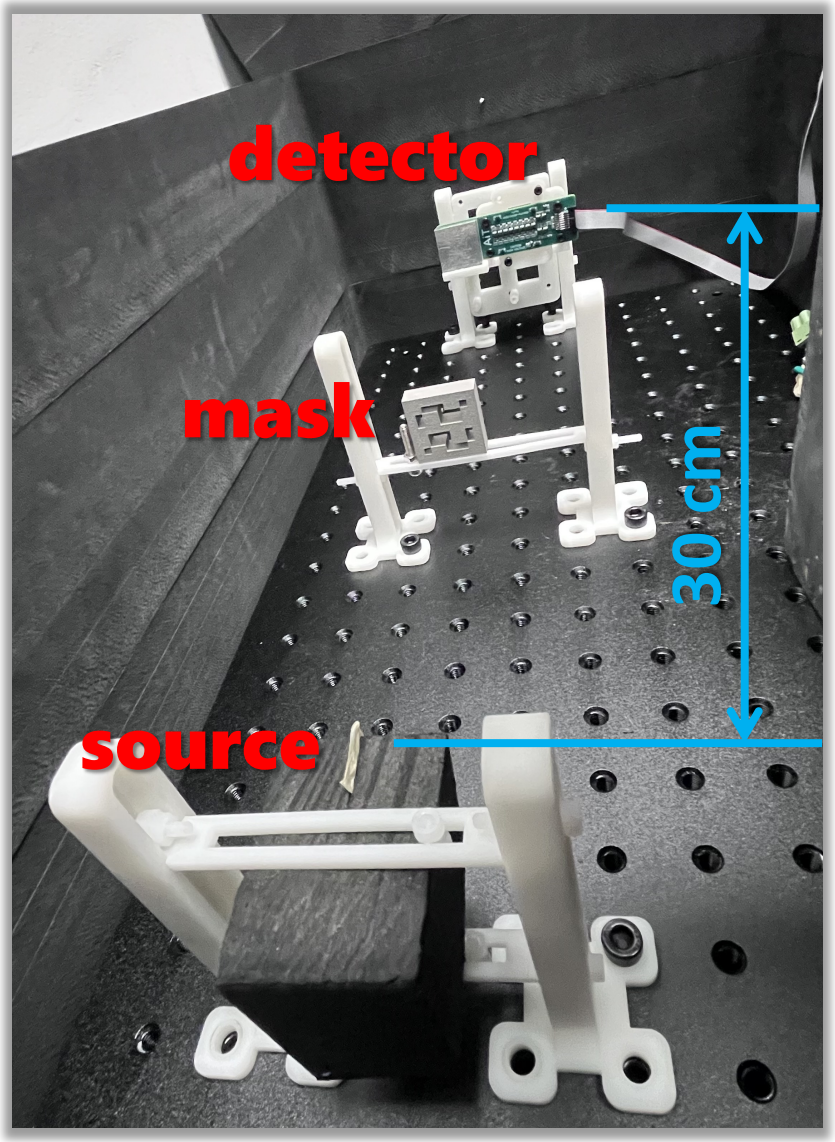

Rank-7 MURA mask

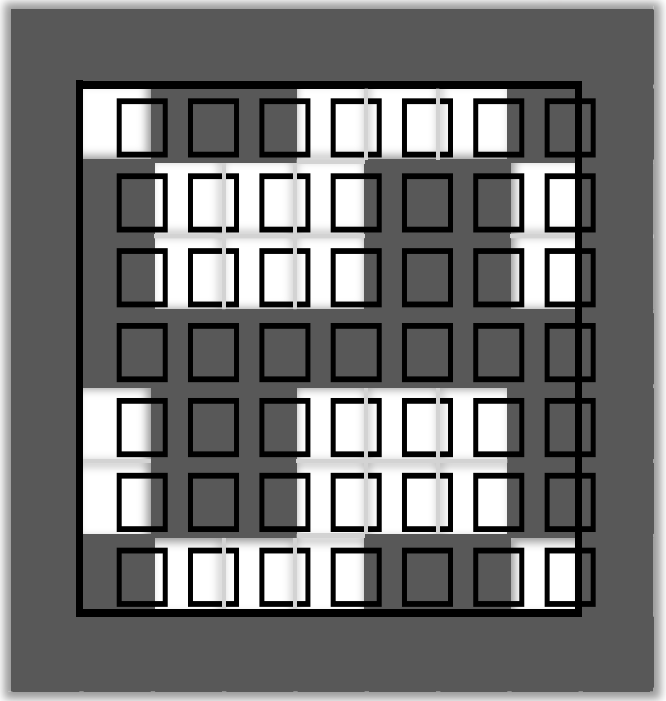

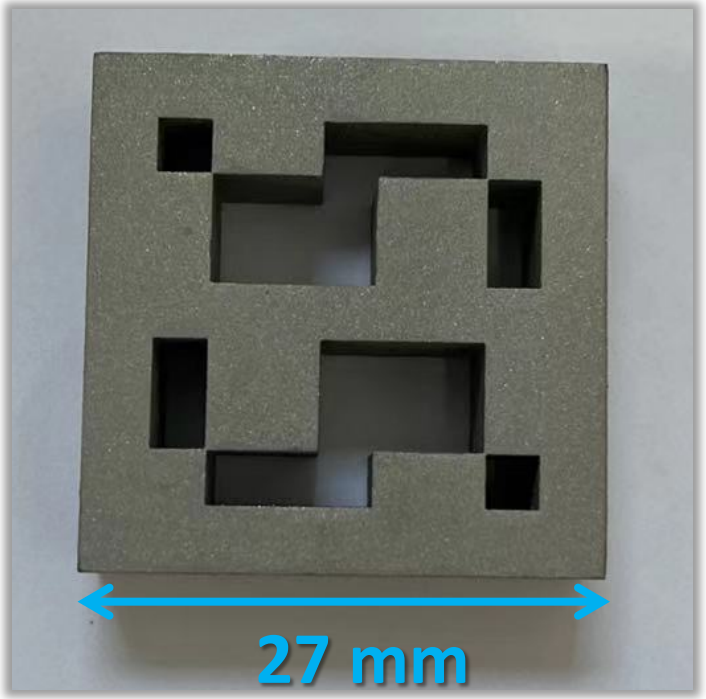

3.2 Single-source measurement

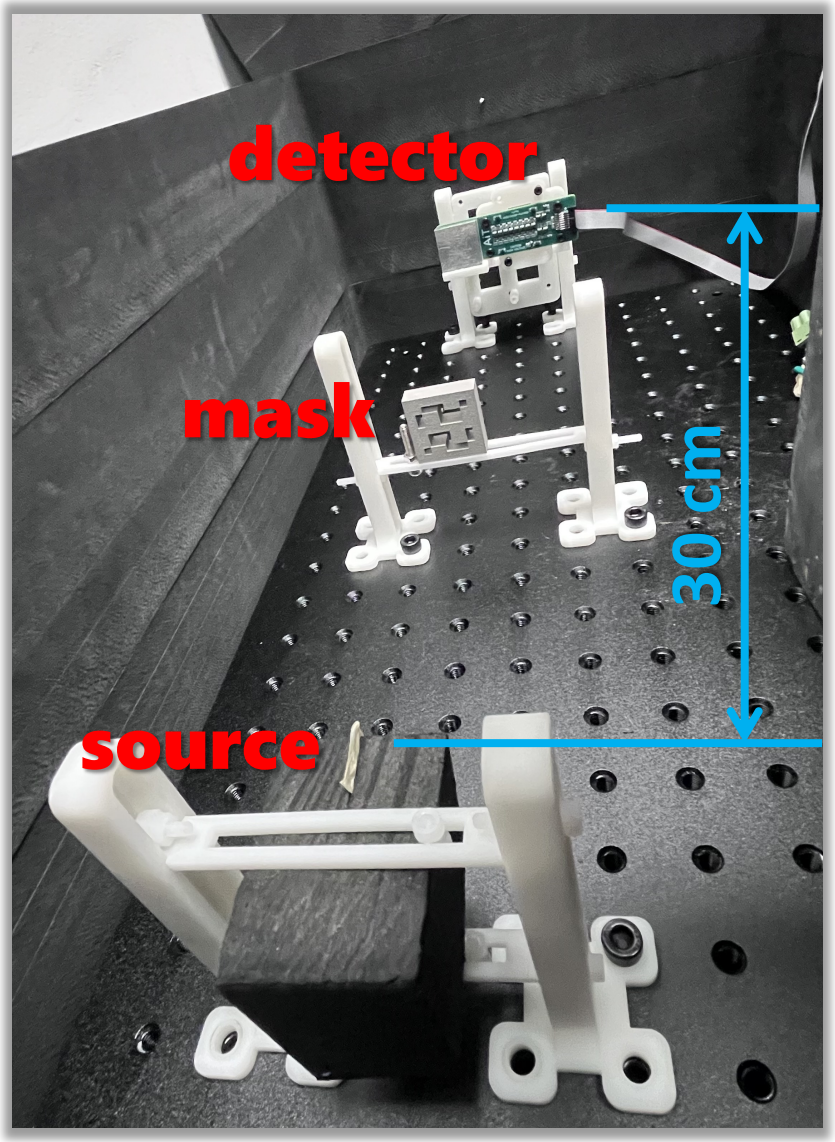

Gamma-ray hit position reconstruction

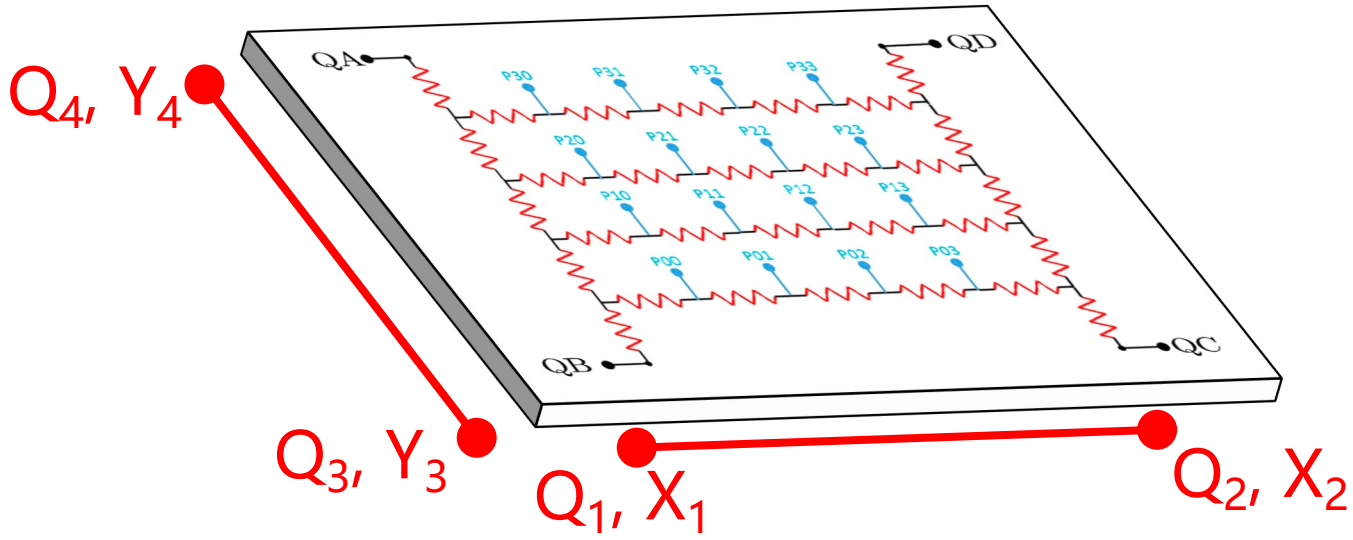

$$\left.\begin{aligned} Q_1 &= Q_A + Q_B \\ Q_2 &= Q_C + Q_D \\ Q_3 &= Q_B + Q_C \\ Q_4 &= Q_A + Q_D \end{aligned}\right\}$$

$$X = \frac{Q_1 \cdot X_1 + Q_2 \cdot X_2}{Q_1 + Q_2}$$

$$Y = \frac{Q_3 \cdot Y_3 + Q_4 \cdot Y_4}{Q_3 + Q_4}$$

3.2 Single-source measurement

Flood map test

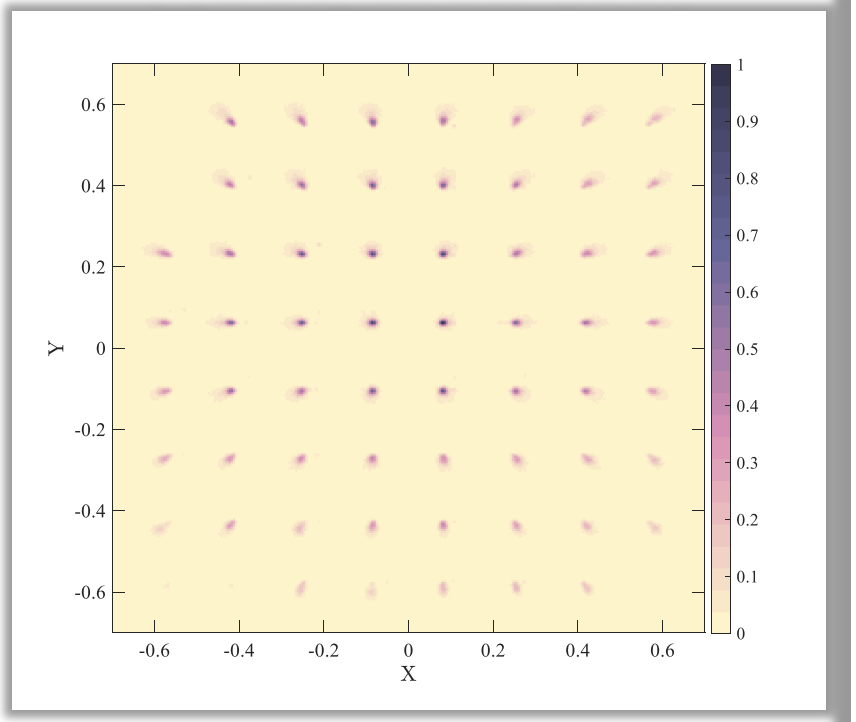

Pulse height spectra in all pixels

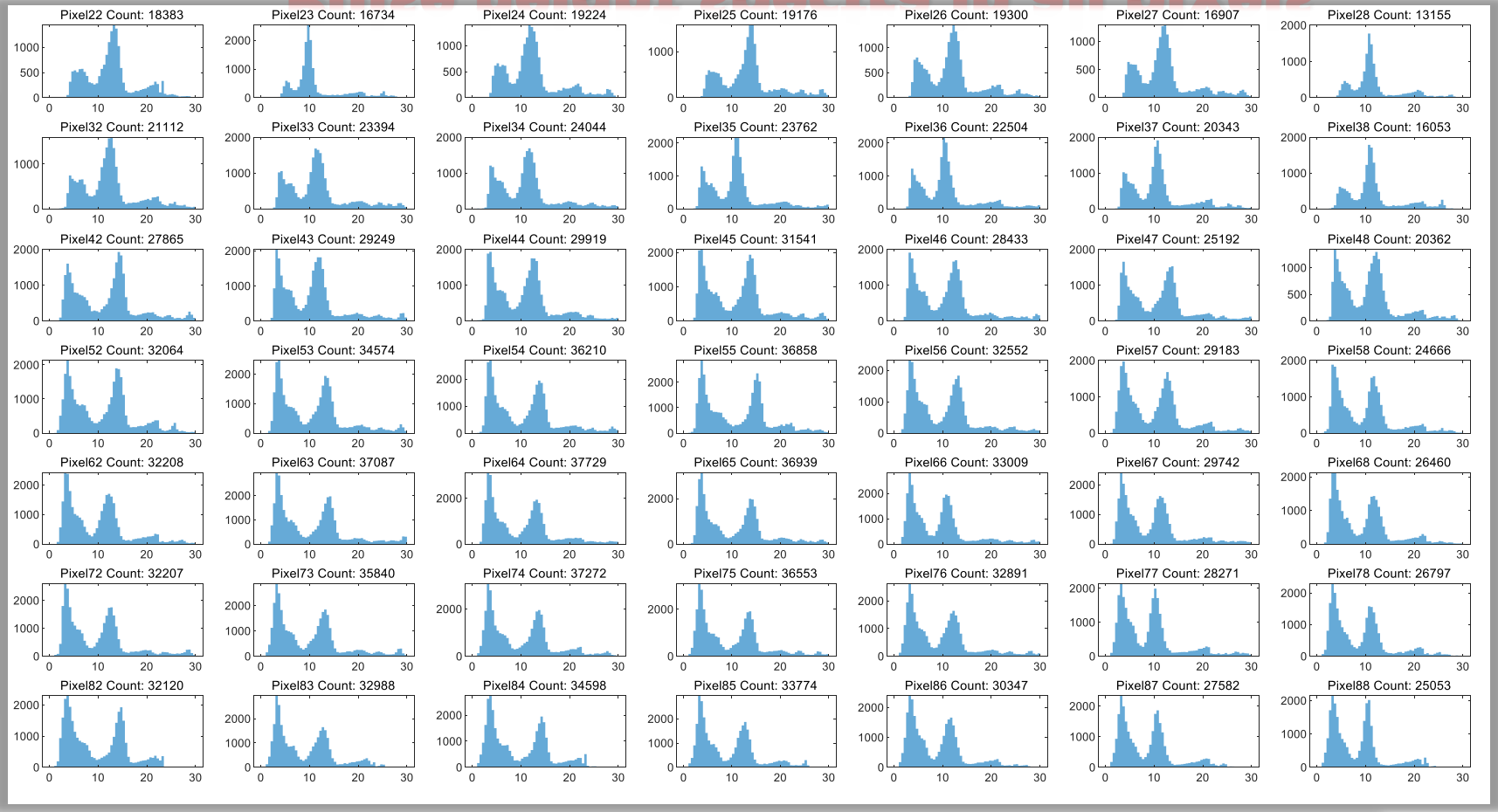

- A double-threshold was used to discriminate and count 0.511-MeV gamma photons.

3.2 Single-source measurement

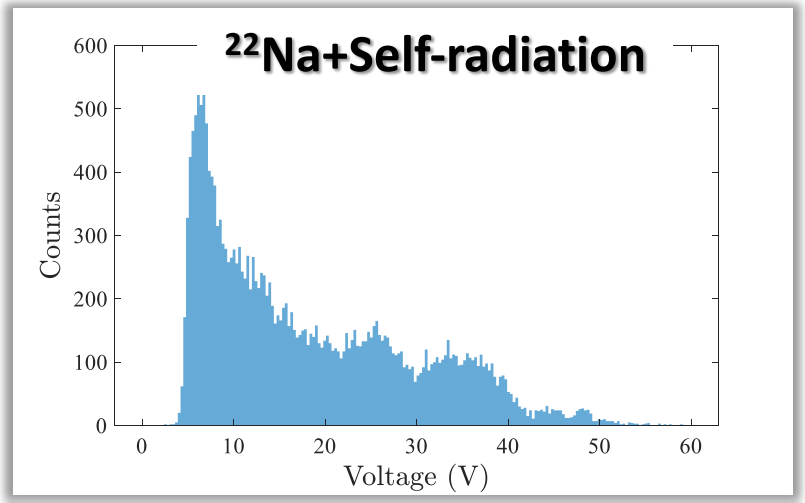

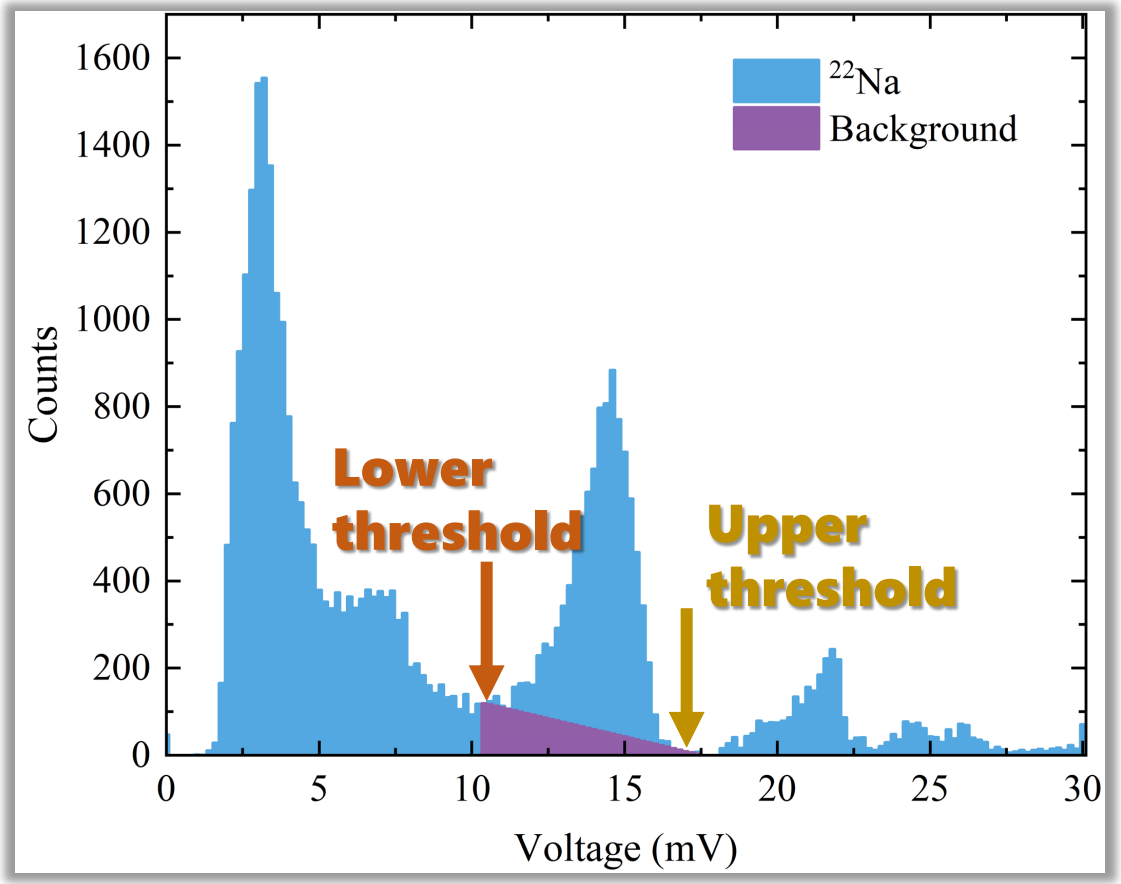

- A double-threshold was used to discriminate 0.511-MeV gamma photons.

3.2 Single-source measurement

Reconstructed images varying source-detector distance

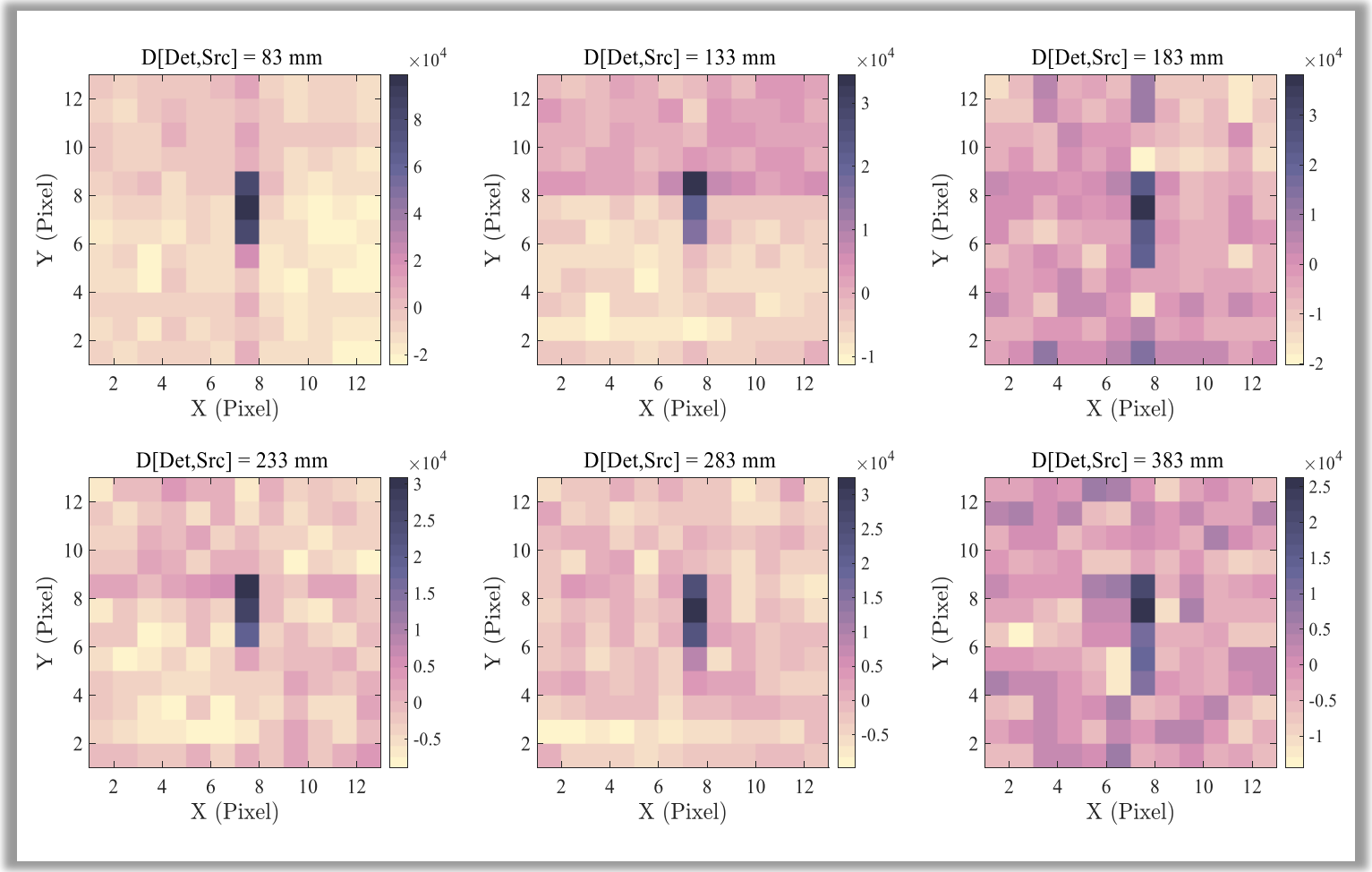

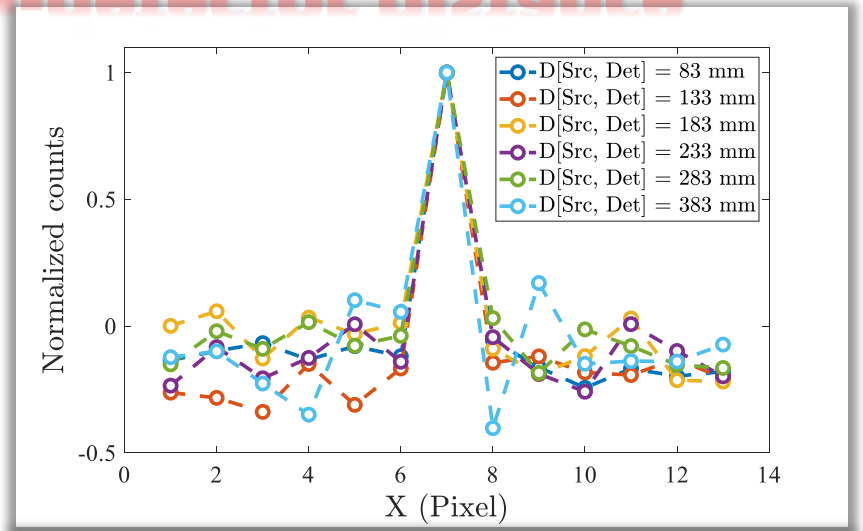

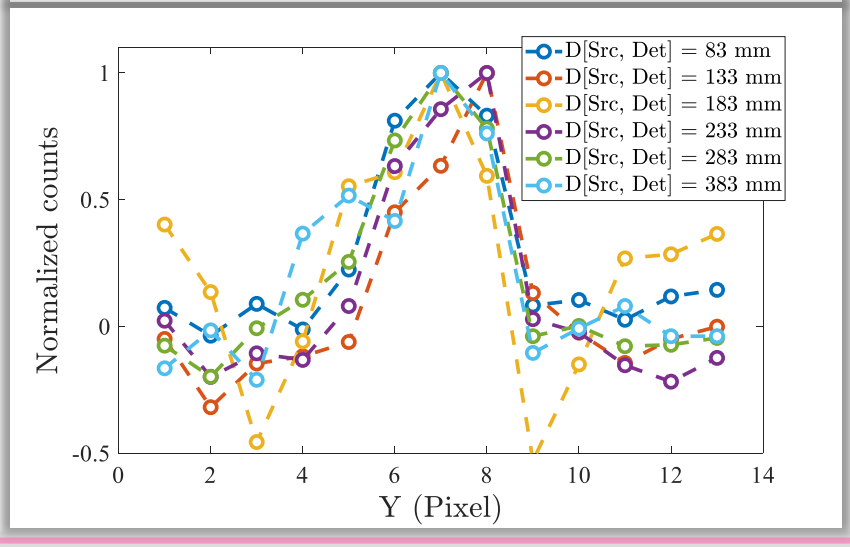

3.3 Double-source measurement

Double ^{22}Na sources

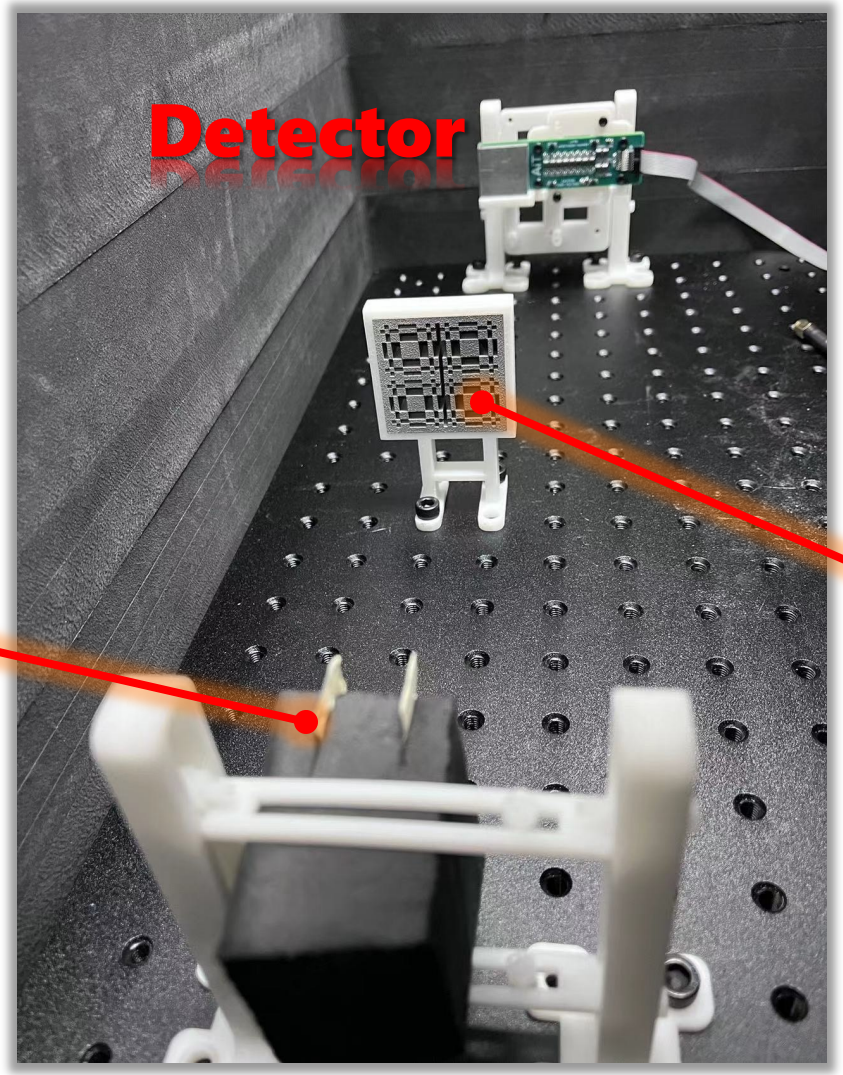

Rank-13 MURA mask

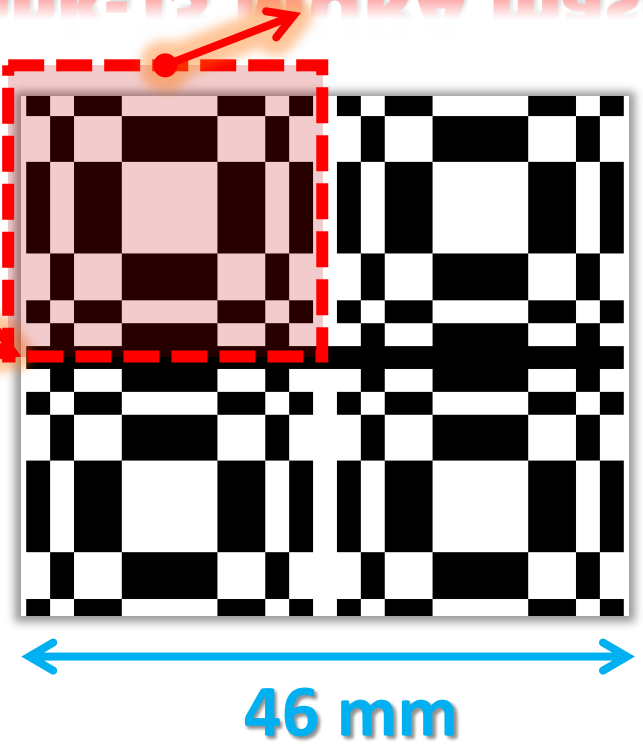

3.3 Double-source measurement

Reconstructed images varying source-detector distance

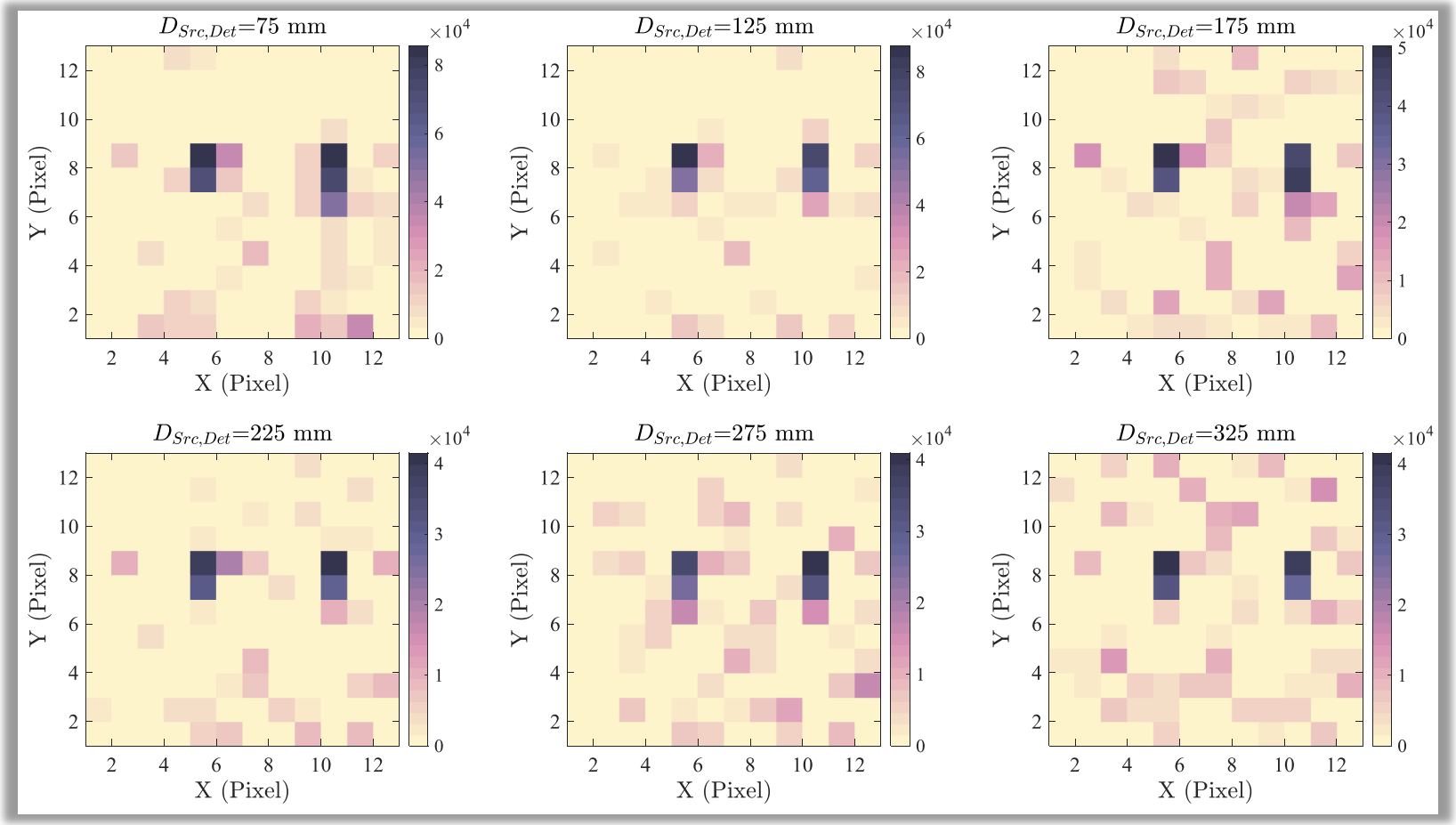

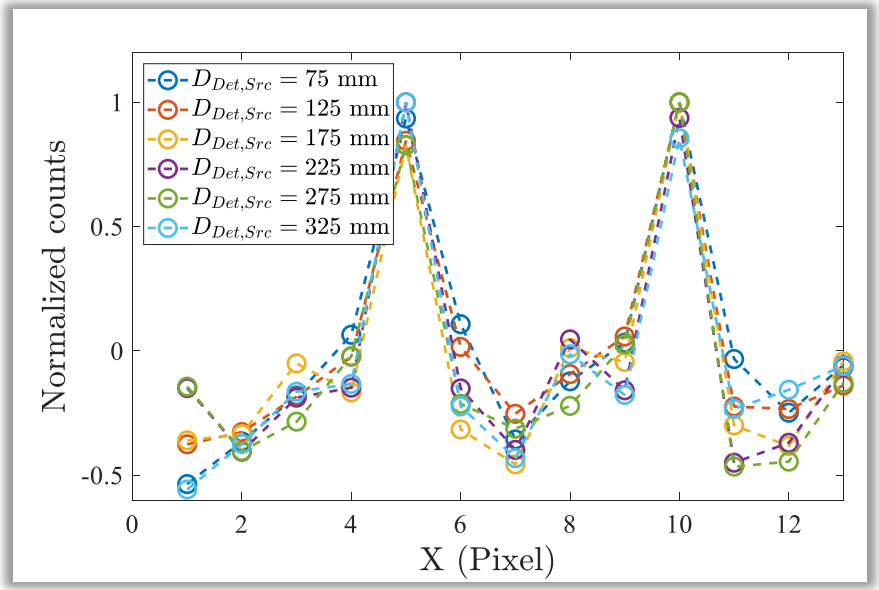


IV. Summary and outlook
All in a muon

4.1 Summary

Simulation

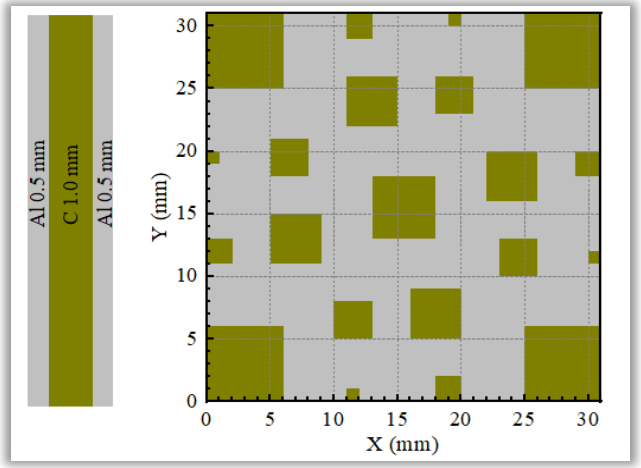

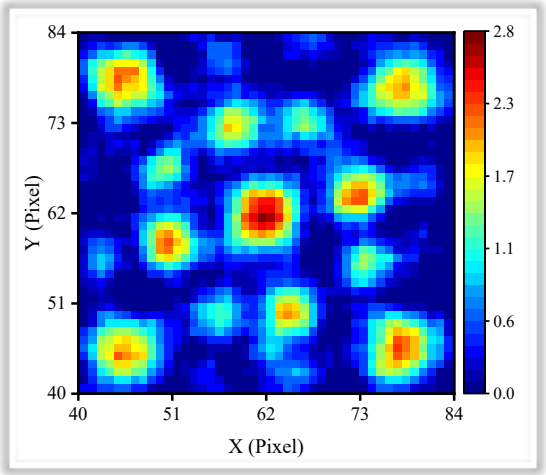

Experiment

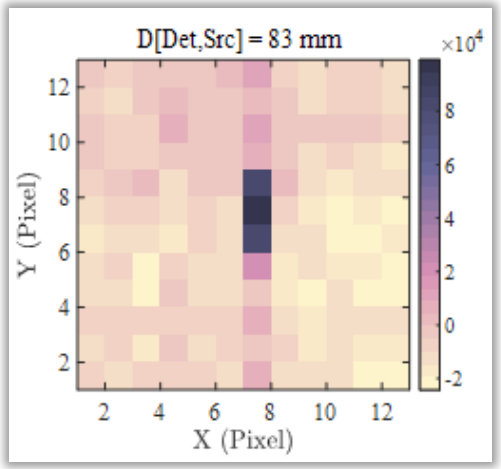

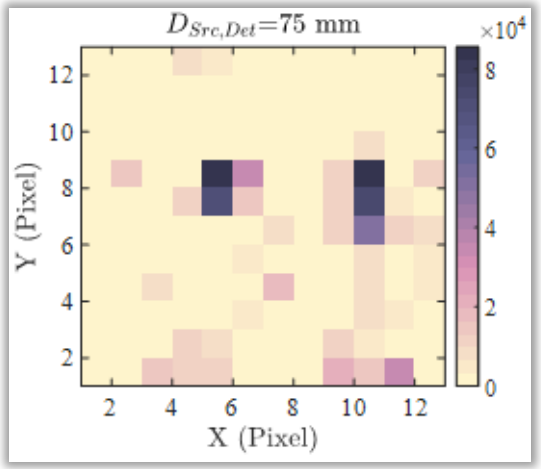

- The feasibility of using the coded aperture imaging method in the field of MIXE imaging was confirmed in Geant4 simulations and alternative experiments
- Due to the usage of a coded mask, its thickness will limit the detectable energy of muonic X-rays. Thus, the observable atomic number is limited.
- The pixel size limits the position resolution of a imaging detection system

4.2 Prospects on instrument developments

Detector

- ✓ CdZnTe: 16×16 cells
- ✓ 1 mm² cell size
- ✓ Signal digitization

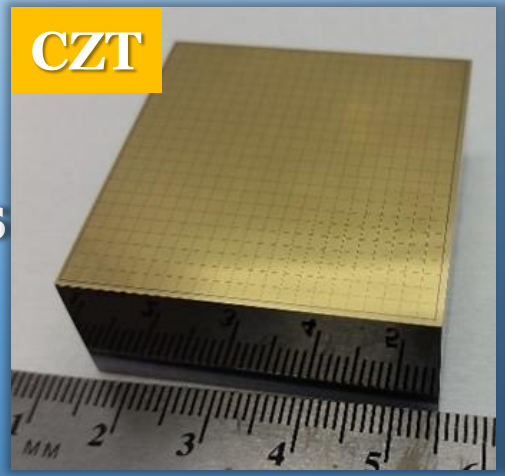

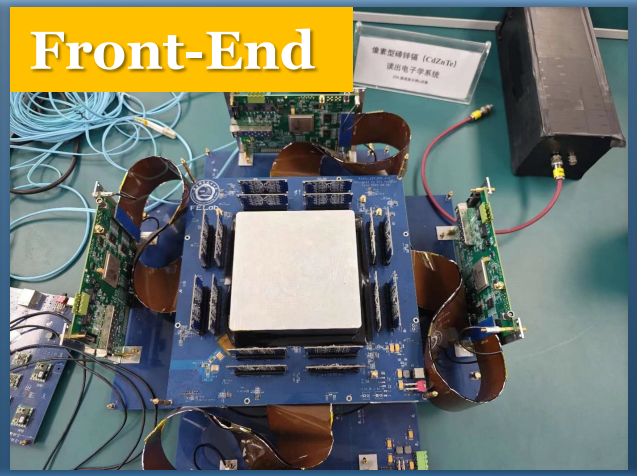

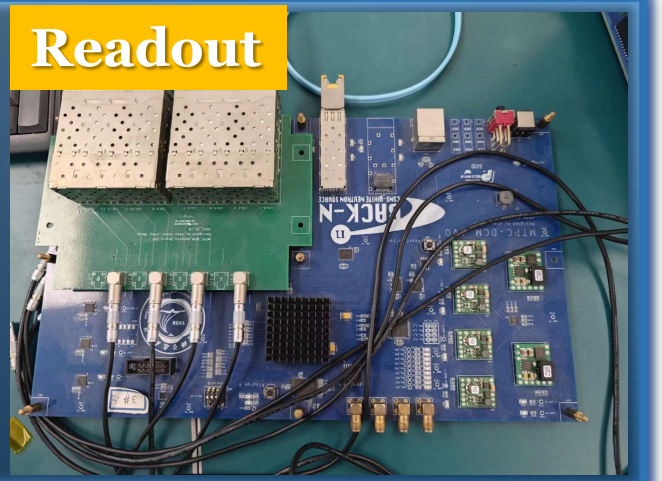

Algorithm

- ✓ Cross-Correlation
- ✓ MLEM/FFT/T2S …
- ✓ Machine learning

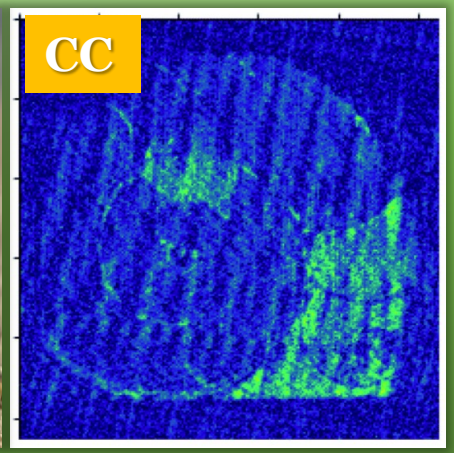

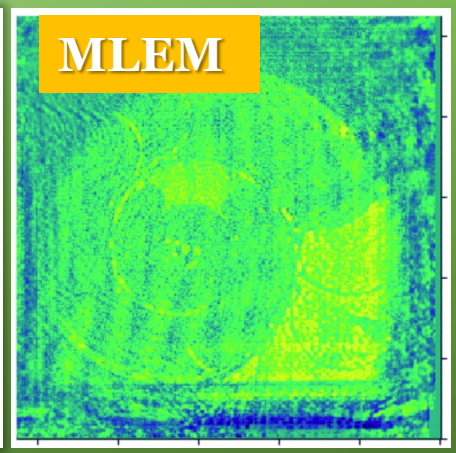

Thanks!

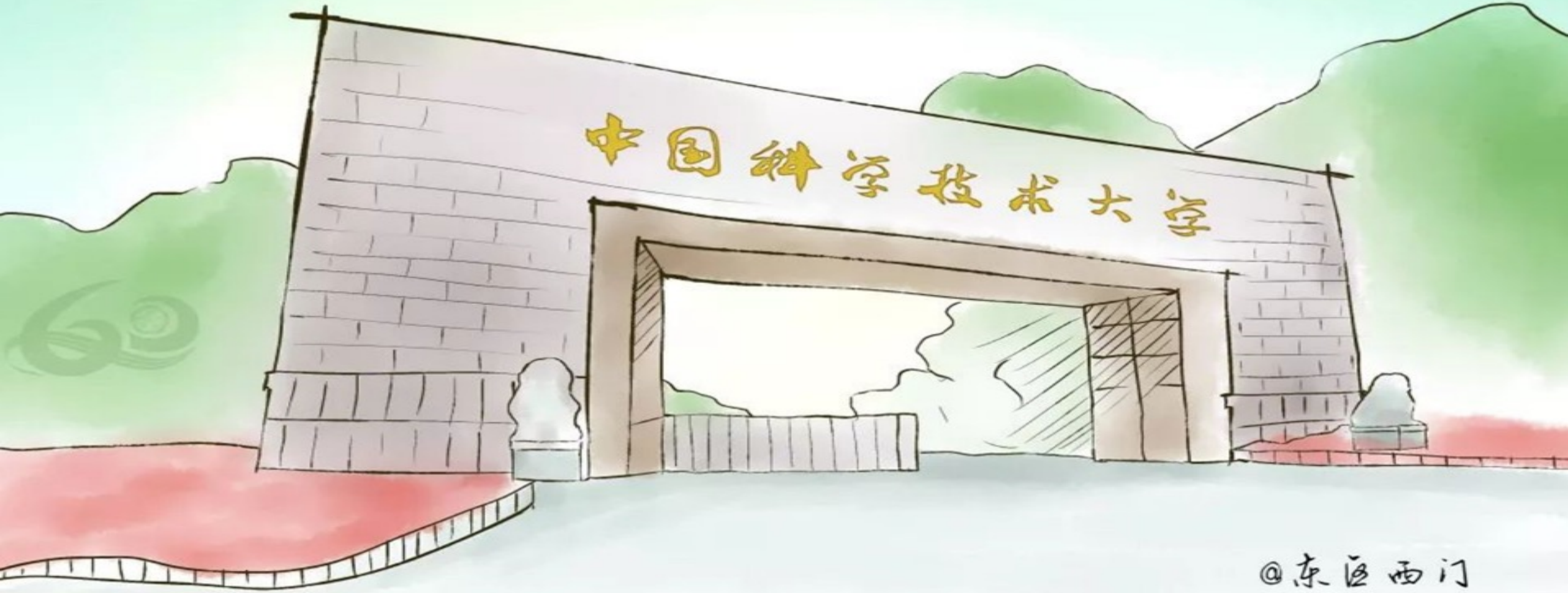

Main Gate of USTC